



**3D PRINTING OF HUMAN ANEURYSM AORTIC ARTERY
USING CT SCAN IMAGES**

MUHAMMAD SHAHRUL RIZAL BIN SARIPUZAN
UNIVERSITI TEKNIKAL MALAYSIA MELAKA B092110231

**BACHELOR OF MECHANICAL ENGINEERING
TECHNOLOGY (MAINTAINANCE TECHNOLOGY) WITH
HONOURS**

2024



Faculty of Mechanical Technology and Engineering

**3D PRINTING OF HUMAN ANEURYSM AORTIC ARTERY USING CT
SCAN IMAGES**

Muhammad Shahrul Rizal Bin Saripuzan

**Bachelor of Mechanical Engineering Technology (Maintenance Technology) with
Honours**

2024

**3D PRINTING OF HUMAN ANEURYSM AORTIC ARTERY USING CT
SCAN IMAGES**

MUHAMMAD SHAHRUL RIZAL BIN SARIPUZAN



A thesis submitted

in fulfilment of the requirements for the degree of

**Bachelor of Mechanical Engineering Technology (Maintenance Technology) with
Honours**

UNIVERSITI TEKNIKAL MALAYSIA MELAKA

Faculty of Mechanical Technology and Engineering

UNIVERSITI TEKNIKAL MALAYSIA MELAKA

2024

DECLARATION

I declare that this Choose an item. entitled “3D Printing of Human Aneurysm Aortic Artery Using CT Scan Images” is the result of my own research except as cited in the references. The Choose an item. has not been accepted for any degree and is not concurrently submitted in candidature of any other degree.

Signature

:

Name

: Muhammad Shahrul Rizal Bin Saripuzan

Date

: 10 January 2025

APPROVAL

I hereby declare that I have checked this thesis, and this thesis is adequate in terms of scope and quality for the award of the Bachelor of Mechanical Engineering Technology (Maintenance Technology) with Honours.

Signature :

Supervisor Name : Dr. AbdulGaphur AbdulKhadar Athani

Date :11 January 2025

DEDICATION

I dedicate this work to the memory of my beloved mother, who passed away in 2022 during my second semester of studies. My compass has been her unfailing confidence and support in all I have attempted, even in my darkest hours. My father and siblings, who have supported and loved me no end on this trip, have my eternal gratitude.

In finishing this project on 3D printing of human aneurysm aortic artery using CT scan pictures, I promised my mother and myself to always aim for the best. I start this project with a lot of attention and resolve, hoping to keep my pledge and do well.



ABSTRACT

Aortic artery aneurysms are a critical condition characterised by the weakening and outward bulging of the aortic wall, necessitating prompt discovery and treatment strategy formulation. This research established a novel process for producing precise patient-specific 3D printed models of aortic aneurysms using CT scan imaging data. The integrated methodology amalgamated cardiovascular computed tomography (CT) with 3D printing for clinical applications, evaluating the efficacy of 3D models in preoperative surgery planning, educational endeavours, and enhanced patient outcomes. The process included image acquisition via high-resolution spiral CT angiography, image segmentation to delineate the aneurysm shape, 3D reconstruction to create a digital model, and 3D printing of the patient-specific physical model. The digital model was transferred into Ansys software for computational fluid dynamics (CFD) simulation to assist the study. This entailed delineating blood characteristics, establishing pragmatic boundary conditions, and modelling blood flow to examine flow patterns, pressure distribution, and wall shear stress. Stringent quality assurance protocols were established to assess segmentation, digital editing, and printing precision. The resultant 3D printed replicas, integrated with CFD data, provided accurate representations of each patient's distinct aortic aneurysm anatomy, allowing for visualisation of the aneurysm and surrounding structures for surgical planning, intervention simulation, and enhancing medical education and patient comprehension. This study illustrated the transformative potential of incorporating 3D printing and CFD analysis into cardiovascular medicine by examining technical aspects, assessing clinical impact, and evaluating economic feasibility. It provides a comprehensive solution for precise anatomical modelling, enhances diagnostic and therapeutic decision-making, and may improve outcomes for patients with aortic aneurysms.

ABSTRAK

Aneurisma aorta adalah keadaan yang mengancam nyawa di mana dinding aorta menjadi lemah dan menonjol keluar, memerlukan pengesanan awal dan perancangan rawatan. Kajian ini membangunkan satu metodologi inovatif untuk menghasilkan model 3D aneurisma aorta khusus pesakit yang tepat menggunakan data imbasan CT. Pendekatan bersepadu ini menggabungkan tomografi berkomputer kardiovaskular (CT) dan percetakan 3D untuk aplikasi klinikal, menilai kegunaan model 3D untuk perancangan pembedahan pra-operasi, tujuan pendidikan, dan meningkatkan hasil pesakit. Metodologi ini merangkumi pemerolehan imej melalui angiografi CT lingkaran resolusi tinggi, segmentasi imej untuk mengasingkan geometri aneurisma, pembinaan semula 3D untuk menghasilkan model digital, dan percetakan 3D model fizikal khusus pesakit. Untuk meningkatkan lagi analisis, model digital diimport ke dalam perisian Ansys untuk simulasi dinamik bendalir pengiraan (CFD). Ini melibatkan penentuan sifat darah, menetapkan keadaan sempadan yang realistik, dan mensimulasikan aliran darah untuk menganalisis corak aliran, taburan tekanan, dan tegasan ricih dinding. Langkah jaminan kualiti yang ketat telah dilaksanakan, menilai segmentasi, penyuntingan digital, dan ketepatan percetakan. Replika bercetak 3D yang terhasil, digabungkan dengan data CFD, menawarkan perwakilan tepat anatomi aneurisma aorta unik setiap pesakit, membolehkan visualisasi aneurisma dan struktur bersebelahan untuk perancangan pembedahan, mensimulasikan intervensi, dan memudahkan pendidikan perubatan dan pemahaman pesakit. Dengan menyiasat aspek teknikal, menilai impak klinikal, dan menilai kebolehlaksanaan ekonomi, kajian ini menunjukkan potensi transformatif menggabungkan percetakan 3D dan analisis CFD ke dalam perubatan kardiovaskular, menawarkan penyelesaian komprehensif untuk pemodelan anatomi yang tepat, meningkatkan pengambilan keputusan diagnostik dan terapeutik, dan berpotensi meningkatkan hasil untuk pesakit dengan aneurisma aorta.

ACKNOWLEDGEMENTS

In the Name of Allah, the Most Gracious, the Most Merciful

With this opportunity, I would want to thank Dr. Abdulghafur, my supervisor.

from the Faculty of Mechanical Technology and Engineering (FTKM) at Universiti Teknikal Malaysia Melaka (UTeM), for his invaluable guidance, encouragement, and support during the completion of this project. His direction has been particularly important in forming this work and my academic career. I also appreciate my colleagues' understanding and assistance during this study project. With gratitude to my cherished family especially my mother, father, and siblings for their unfailing support and encouragement throughout my academic career. Finally, I would want to thank everyone who has participated in this effort, either directly or indirectly. This work has happened in large part because of your contribution.

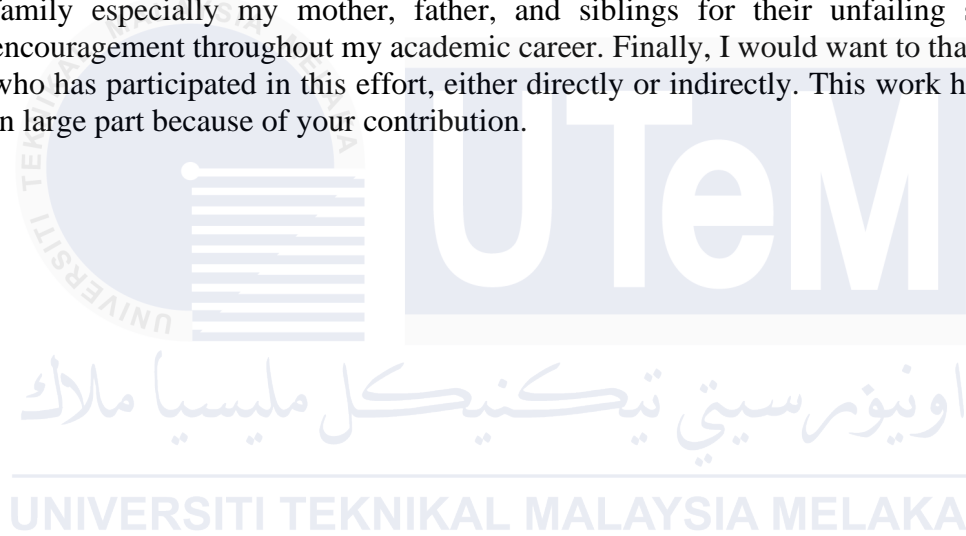


TABLE OF CONTENTS

	PAGE
DECLARATION	
APPROVAL	
DEDICATION	
ABSTRACT	i
ABSTRAK	ii
ACKNOWLEDGEMENTS	iii
TABLE OF CONTENTS	iv
LIST OF TABLES	vi
LIST OF FIGURES	vii
LIST OF SYMBOLS AND ABBREVIATIONS	viii
CHAPTER 1 INTRODUCTION	4
1.1 Background	4
1.2 Problem Statement	4
1.3 Research Objective	5
1.4 Scope of Research	6
CHAPTER 2 LITERATURE REVIEW	7
2.1 Introduction	7
2.2 Error! Reference source not found.	7
2.2.1 What is the human aorta (aortic artery)?	8
2.2.2 How do aortic aneurysms occur?	13
2.2.3 Treatment for Aortic Aneurysms	13
2.3 Cardiovascular Computed Tomography Angiography (CCTA)	14
2.3.1 What is Computed Tomography (CT)?	15
2.3.2 How does a CT scan work?	16
2.3.3 What are the key components and principles of a CT scan?	16
2.3.4 Certification for Cardiovascular Computed Tomography (CCT)	22
2.4 Three-dimensional (3D) Printed Model	25
2.4.1 The Origin of 3D Printing Techniques	26
2.4.2 What is 3D Printing? How does it work?	28
2.5 Acts & Legislation in Medical 3D-Printed Models	36

2.5.1	European Union (EU)	36
2.5.2	United States Food & Drug Administration	39
2.6	Summary or Research Gap	42
CHAPTER 3	METHODOLOGY	44
3.1	Introduction	44
3.2	Research Design	45
3.3	Proposed Methodology	45
3.3.1	Experimental Setup for 3D Printed Models from CT scan images	46
3.4	Limitation of Proposed Methodology	51
3.5	Summary	52
CHAPTER 4	RESULTS AND DISCUSSIONS	66
4.1	Introduction	53
4.2	3D-Printed Model of Patient-Specific Aortic Artery Aneurysms	54
4.3	3D Printed Model	61
4.4	CAD Model Preparation and Comparison by CFD Analysis	61
CHAPTER 5	CONCLUSION	66
REFERENCES		80

LIST OF TABLES

TABLE	TITLE	PAGE
Table 2.1	Summary of Independent Practitioner (IP) and Advanced Practitioner (AP) capabilities upon completion of training	22
Table 2.2	IPR types, subject matter, and purpose	50
Table 2.3	Earlier Version of FDA's Framework Included Manufacturing Scenarios for 3DPOC	52
Table 2.4	Updated Version of FDA's Framework Now Consists of 3 Scenarios for 3DPOC	53
Table 3.1	The table summarizes essential parameters for 3D printing, including design, material, printer, post-processing, application-specific, quality control, software, regulatory, and environmental aspects	61
Table 3.2	summarises the equipment and tools necessary for efficiently and accurately 3D printing a human aneurysm aortic artery from CT scanner images, meeting both research and clinical application requirements.	63
Table 4.1	Shows the front view, top view, and right view of the Aneurysm Aorta	71
Table 4.2	Shows the front view, top view and right view of the Normal Aorta	

LIST OF FIGURES

FIGURE	TITLE	PAGE
Figure 2.1	An illustration of the human aorta	6
Figure 2.2	An illustration of aortic aneurysms occurrence that affected by Marfan Syndrome	8
Figure 2.3	An Infographic on how Penetrating Atherosclerotic Ulceration Develop in the Human Aorta	10
Figure 2.4	Shows the differences between aneurysm and pseudoaneurysm	10
Figure 2.5	A prime illustration of a thoracic aorta that is healthy and one that has an aneurysm	11
Figure 2.6	A diagram of a healthy compared to bicuspid aortic valve	12
Figure 2.7	The illustration shows the placement of a stent graft in an abdominal	13
Figure 2.8	An example of Cardiac Computed Tomography Angiography (CCTA) or Cardiac CT scan	15
Figure 2.9	A computed tomography (CT) scan of a human heart rendered using (a) gradient-based diffuse shading, (b) our method using local visibility, and (c) our method using global visibility.	17
Figure 2.10	Patient in CT Imaging System	18
Figure 2.11	Slice of CT Scanner	19
Figure 2.12	CT Scanner	20
Figure 2.13	CT Scanner Control Room	20
Figure 2.14	SLA-1, the first commercial prototyping device from 3D Systems	28
Figure 2.15	The machine on the left produced all the plastic parts for the machine on the right. Adrian Bowyer (left) and Vik Olliver (right) are members of the RepRap project	30
Figure 2.16	An example of a workflow for CT Scan images to 3D CAD Design of a bottle/jar	33

Figure 2.17	A CT scan of a Spine, made up of many 2D “slices”	34
Figure 2.18	3D Printed Model of a spine section	34
Figure 2.19	shows a general workflow in 3D printing	35
Figure 2.20	A process description of clinical 3D printing. Parallelograms serve as symbols for real-world objects, software, documents, and data, while rectangles serve as descriptions of various process steps. Each of these steps contributes to the final quality of the product. A 5-step classification of the various processes is presented on the left	38
Figure 4.1	shows the flowchart of the whole process	69
Figure 4.2	shows the CT Scan of images of Human Normal Aorta (Left) and Aneurysm Aorta (Right)	
Figure 4.3	shows the interface of MIMICS software and how the image segmented	71
Figure 4.4	illustrates how the 3D model was reconstructed.	
Figure 4.5	shows the support making process for 3D Printing	73
Figure 4.6	shows a flowchart of the 3D Printing Process	74
Figure 4.7	shows the documentation for each part of the 3D Printing Process	75
Figure 4.8	shows the Post-Processing Activities	
Figure 4.9	shows The final replicas from 3D Printing.	76
Figure 4.10	A summary of setup in the ANSYS Fluent	79
Figure 4.11	shows the Wall Shear Stress Contours for Aneurysm Aorta (Left) and Normal aorta (Right)	80

LIST OF SYMBOLS AND ABBREVIATIONS

CAD	-	Computer-aided design
CAPA	-	Corrective and preventive action
3D	-	Three-dimensional
EVAR	-	Endovascular aneurysm repair
CCTA	-	Cardiovascular Computed Tomography Angiography
MDCT	-	Multidetector CT
CT	-	Computed Tomography
SLA	-	Stereolithography
SLS	-	Selective Laser Sintering
FDM	-	Fused Deposition Modelling
FFF	-	Fused Filament Fabrication
CAD	-	Computer-Aided Design
STL	-	Stereolithography file format
MRI	-	Magnetic Resonance Imaging
DICOM	-	Digital Imaging and Communications in Medicine
CAM	-	Computer-Aided Manufacturing
EU	-	European Union
FDA	-	Food and Drug Administration
ASME	-	American Society of Mechanical Engineers
CDRH	-	Center for Devices and Radiological Health
CDER	-	Center for Drug Evaluation and Research
MDR	-	Medical Device Regulation
GDPR	-	General Data Protection Regulation
CJEU	-	Court of Justice of the European Union
IPR	-	Intellectual Property Rights
E&L	-	Exceptions and Limitations
BAV	-	Bicuspid Aortic Valve
MDPS	-	Medical Device Production System
ACR	-	American College of Radiology
AMA	-	American Medical Association
CPT	-	Current Procedural Terminology

CHAPTER 1

INTRODUCTION

1.1 Background

Transporting oxygenated blood to organs and tissues is a critical function of the aorta, the largest artery in the human body. The structure of this object is composed of separate layers that enable it to endure the tremendous force exerted by blood expelled from the heart. However, aortic aneurysms can develop due to a range of conditions such as degenerative disorders, connective tissue abnormalities, and valve defects. These aneurysms are characterised by the weakening and thinning of the aortic wall, posing a potentially life-threatening problem.

Early detection is crucial, and methods like cardiovascular computed tomography angiography (CCTA) have become valuable instruments, employing X-rays to generate accurate, intricate 3D visuals of the heart and its connected blood vessels without the requirement of invasive procedures. Treatment options for aortic aneurysms consist of endovascular aneurysm repair (EVAR), which is a minimally invasive procedure that involves inserting a stent graft through blood vessels, and open aneurysm surgery, a more extensive operation that aims to prevent rupture or dissection by removing and replacing the damaged portion of the aorta with a synthetic fabric tube.

The integration of medical imaging and 3D printing technologies in clinical practice shows exciting potential for improving diagnostic accuracy, surgical planning, and patient outcomes. Nevertheless, the widespread implementation of these innovative techniques encounters obstacles such as inflated costs, the absence of standardised training programmes, and the requirement for a comprehensive approach that effectively integrates these methods into regular clinical workflows.

1.2 Problem Statement

A significant amount of study has been conducted on the capacity of 3D printing to create accurate anatomical models. However, there is limited evidence regarding its long-term advantages and cost-effectiveness in clinical settings, especially in different healthcare

environments. Existing research has not sufficiently addressed the full incorporation of 3D printing and cardiovascular computed tomography (CCT) into standard clinical procedures.

The extensive investigation of the potential of 3D-printed models for surgical planning and education, as well as their impact on long-term patient outcomes and cost-effectiveness, has been lacking. Moreover, the absence of standardised training programmes for medical professionals to proficiently employ these innovative technologies impedes their widespread acceptance and optimal utilisation.

1.3 Research Objective

This study seeks to improve the educational experience for students, researchers, and academics in the medical domain by employing 3D printing technology and computational fluid dynamics (CFD) to visualise and analyse aorta artery aneurysms (AAA). The research aims are as follows:

- a) Convert CT scan data into a 3D printable STL file format. This entails utilising software to analyse CT scan pictures and generate a 3D model suitable for printing. The resultant STL file will be utilised to build instructional 3D printed models of the aorta.
- b) Three-dimensional prints at least two models for comparative analysis: one depicting a normal aorta and the other illustrating an aorta with an aneurysm. This will facilitate a visible and physical comparison of the two circumstances, enhancing the comprehension of the anatomical variations induced by the aneurysm.
- c) Employ computational fluid dynamics (CFD) studies to illustrate the impact of an aneurysm on haemodynamic. This entails modelling blood flow in both normal and aneurysmal aorta models to visualise and analyse variations in velocity, pressure, and wall shear stress. The CFD results will elucidate the haemodynamic changes linked to AAA, hence enriching the educational experience for students, researchers, and scholars.

1.4 Scope of Research

This study will concentrate on formulating and enhancing a system for producing 3D-printed representations of human aortic artery aneurysms utilising CT scanning pictures. This entails investigating diverse methodologies for image segmentation, data processing, and three-dimensional modelling to ensure precise reproduction of patient-specific anatomical characteristics. The objective of the study is to enhance the process by testing several methods to achieve the highest degree of authenticity in printed models.

This study critically evaluates the effectiveness of 3D-printed models in preoperative planning for surgeries involving aortic artery aneurysms. The study will examine the efficacy of these models in enhancing surgical visualisation and procedural understanding by qualitative and quantitative evaluations, including comparisons with current 2D imaging techniques. The research seeks to assess the significance of integrating 3D-printed models into the preoperative workflow by evaluating their influence on surgical decision-making and outcomes.

This project will examine the economic and logistical viability of integrating 3D printing into clinical practice for aortic artery aneurysms, alongside technological considerations. Cost-effectiveness, technological accessibility, and production scalability will be studied to evaluate the feasibility of widespread adoption. By taking these elements into consideration, the study aims to elucidate the real-world consequences of integrating 3D printing into the treatment of this condition, encompassing implications for healthcare delivery and resource allocation.

CHAPTER 2

LITERATURE REVIEW

2.1 Introduction

The Aortic artery aneurysms (AAA) are a critical vascular condition characterized by the weakening and outward bulging of a segment of the aorta, the principal artery of the body. These aneurysms present a significant health risk, as untreated, the compromised aortic wall may rupture, resulting in significant internal hemorrhaging. Precise and thorough visualization of these intricate anatomical structures is essential for effective diagnosis, treatment planning, and patient education.

Historically, cardiovascular computed tomography angiography (CCTA) has been used to image and evaluate AAAs, but it provides limited information in a two-dimensional format, which is particularly relevant in the context of intricate surgical repairs or endovascular interventions. This research investigates the use of 3D printing technology to produce patient-specific models of AAAs based on CT scan data, addressing the limitations of 2D imaging.

The process involves high-resolution CT scans of the patient's aorta, image processing software, and a high-resolution 3D printer. The model is then transformed into a file format suitable for 3D printing, and post-processing procedures may be required.

The advantages of 3D printed aneurysm models extend beyond surgical preparation. They serve as effective tools for patient education, enhancing communication between physicians and patients, improving understanding of treatment alternatives, and potentially alleviating anxiety related to diagnosis and treatment. Additionally, 3D printed models can be used as training tools for surgeons, particularly in endovascular repair.

2.1.1 What is the human aorta (aortic artery)?

The aorta is the largest artery in the human body. The aortic arch commences at the aortic orifice of the aortic valve and terminates at the fourth lumbar vertebra. The primary function of the aorta is to convey oxygenated blood, or oxyhaemoglobin, to nourish all organs and cells. As a person ages, the structure of the aorta undergoes progressive alterations. The diameter of the aorta, its thickness, microstructural components, and other anatomical factors.

The aorta is segmented into four sections: the ascending aorta, the aortic arch, the descending aorta, and the abdominal aorta. Each component is interconnected and functions as the primary pump in the human circulatory system. The aorta consists of a thin layer known as the tunica intima, a thick elastic middle layer referred to as the tunica media, and a thin outer layer called the tunica adventitia. The layers enable the aorta to absorb the force of blood as it is propelled from the heart to the entire body (Dr. Paulien Moyaert, 2023). Figure 2.1 presents a two-dimensional depiction of the human aorta.

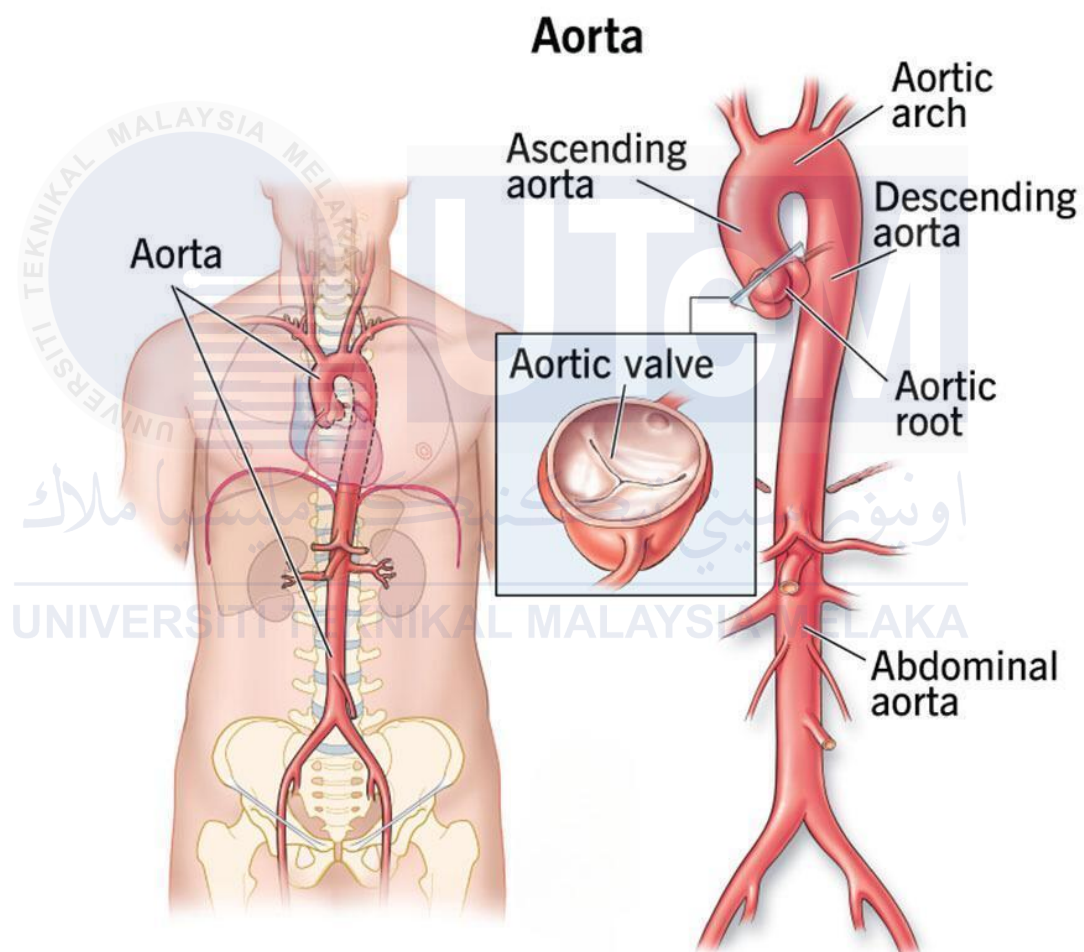


Figure 2.1 An illustration of the human aorta

2.1.2 How do aortic aneurysms occur?

Aortic aneurysms can arise from multiple factors or causes. The initial type is degenerative aortic aneurysms. Degenerative aortic aneurysms represent the

predominant category of aneurysms. They arise when the connective tissue and muscular layer of the aorta deteriorate and thin, heightening the risk of rupture or dissection (Söreljus et al., 2023). Degenerative aortic aneurysms frequently occur in the abdominal region or the descending thoracic aorta.

The third item on the list is Marfan syndrome and connective tissue disorders. Marfan syndrome is an uncommon genetic mutation that impacts the body's connective tissue and various organs. This may result in aortic enlargement, or dilation of the aorta, which can be fatal (Mubarik, Sharma, & Law, 2023). Typically, Marfan syndrome patients experience aneurysms at the aortic root, although they may also occur in the descending thoracic aorta or the abdominal region. The aortic wall's strength is derived from connective tissue; thus, a compromised aortic wall may result in an aneurysm, which has the potential to tear or rupture (Types and Causes of Aortic Aneurysms, n.d.). Figure 2.2 offers further elucidation on the sensations experienced by the heart in the context of Marfan syndrome.

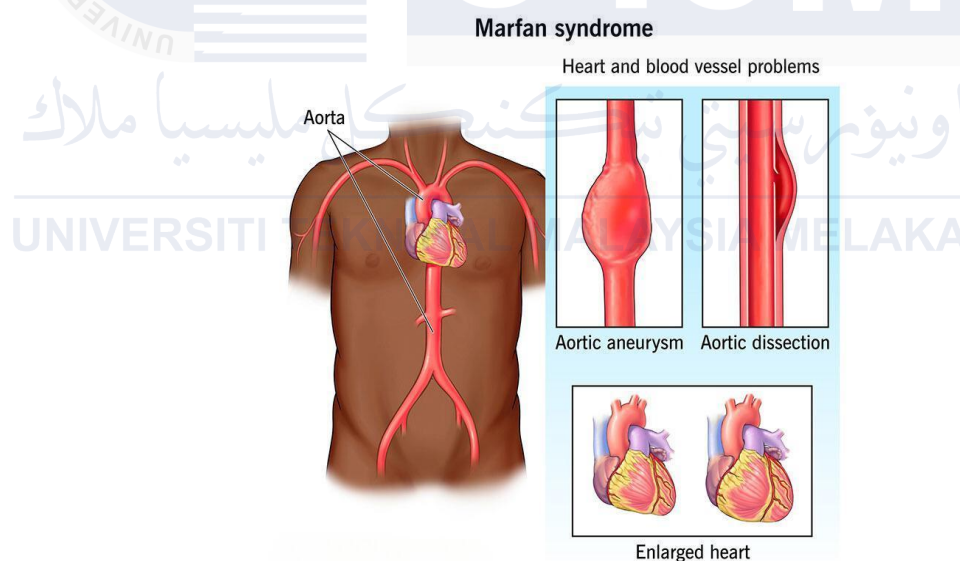


Figure 2.2 An illustration of aortic aneurysms occurrence that affected by Marfan Syndrome

The next one is penetrating atherosclerotic ulceration. Penetrating atherosclerotic ulceration occurs when cholesterol plaque develops in the arteries, causing them to enlarge or develop holes in the aortic wall (Söreljus et al., 2023). It can also allow blood to leak outside the artery and pool into a hematoma, or clot, which can cause pain or

swelling. This syndrome typically happens in older patients and often affects the descending thoracic aorta, though it can also develop in the aorta. When this occurs, patients often experience chest pain. Penetrating atherosclerotic ulceration can also arise without symptoms. Figure 2.3 shows how this disease develops over time.

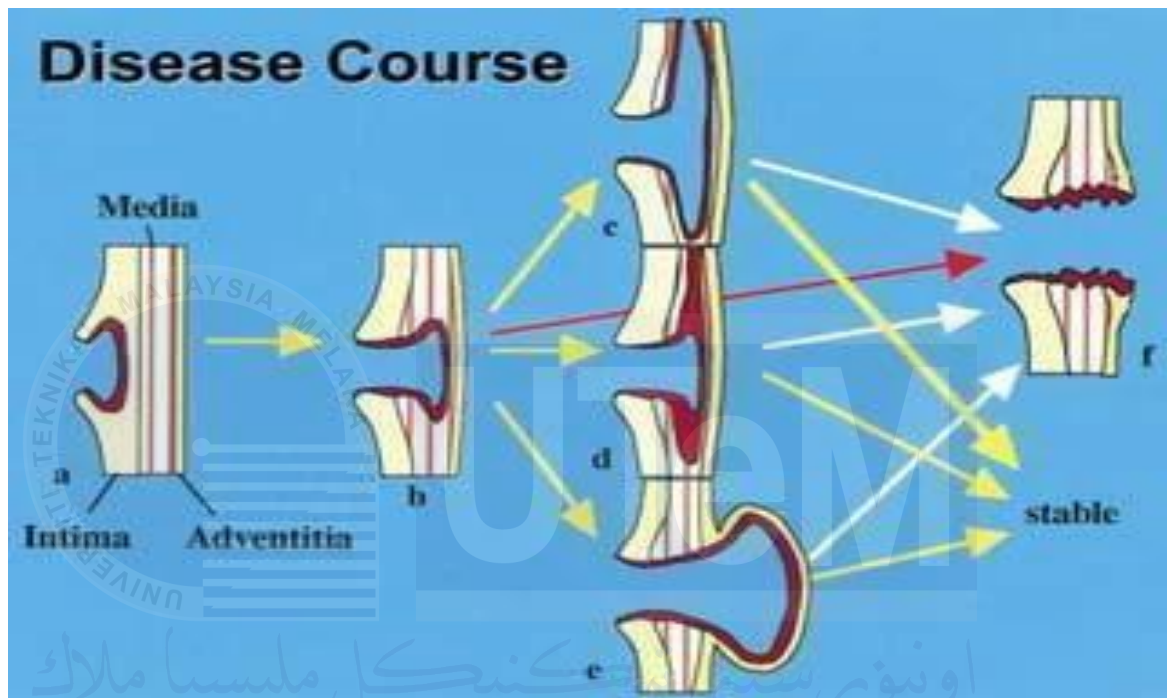


Figure 2.3 An Infographic on how Penetrating Atherosclerotic Ulceration Develop in the Human Aorta

The next one is pseudonymised. A pseudoaneurysm, also referred to as a false aneurysm, typically results from damage to the aortic wall and causes blood clots outside the outer layer of the wall rather than within the layers of the wall (Sörelis et al., 2023). Patients may experience pain as the expanded aorta presses on the patient's other organs. We diagnose this condition with a computerised tomography or magnetic resonance imaging scan (Cardiac Computed Tomography Angiography, 2023).

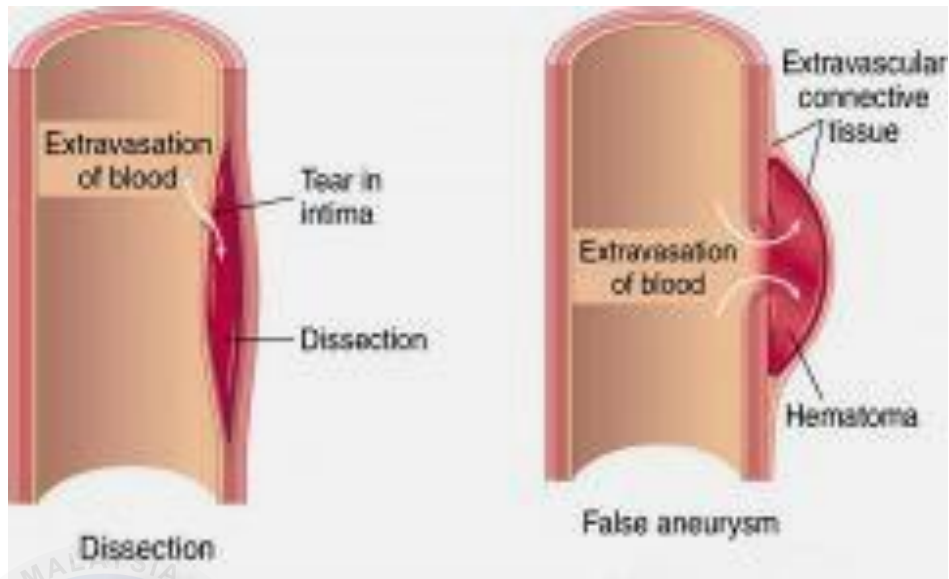


Figure 2.4 Shows the differences between aneurysm and pseudoaneurysm

The next one is thoracic aortic aneurysms. Thoracic aortic aneurysms occur in the arteries that go through the patient's chest area. This is a rare disease that affects more men than women (Sörelis et al., 2023). It is linked to chronic obstructive pulmonary disease, genetics, smoking, and high blood pressure. Not all thoracic aortic aneurysms have the same implications, and therefore treatment options vary. Given the risk of rupture, it is advisable to be more concerned about thoracic aortic aneurysms that are growing quickly than those that are growing more slowly)

Thoracic Aortic Aneurysm

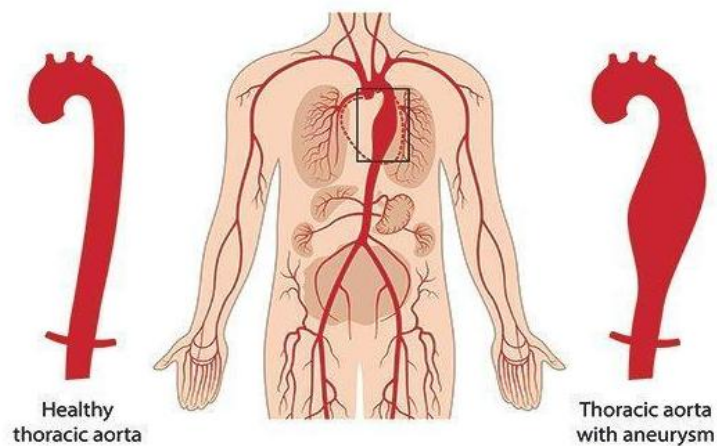


Figure 2.5 A prime illustration of a thoracic aorta that is healthy and one that has an aneurysm

The last one is bicuspid aortic valve disorder (BAV). A bicuspid aortic valve is a common congenital heart defect in which the bicuspid aortic valve contains two cusps instead of the usual three. This leads to degenerative changes of the valve and is associated with dilation of the aorta (Mubarik, Sharma, & Law, 2023). Figure 2.6 shows a comparison between a normal aortic valve and a bicuspid aortic valve.

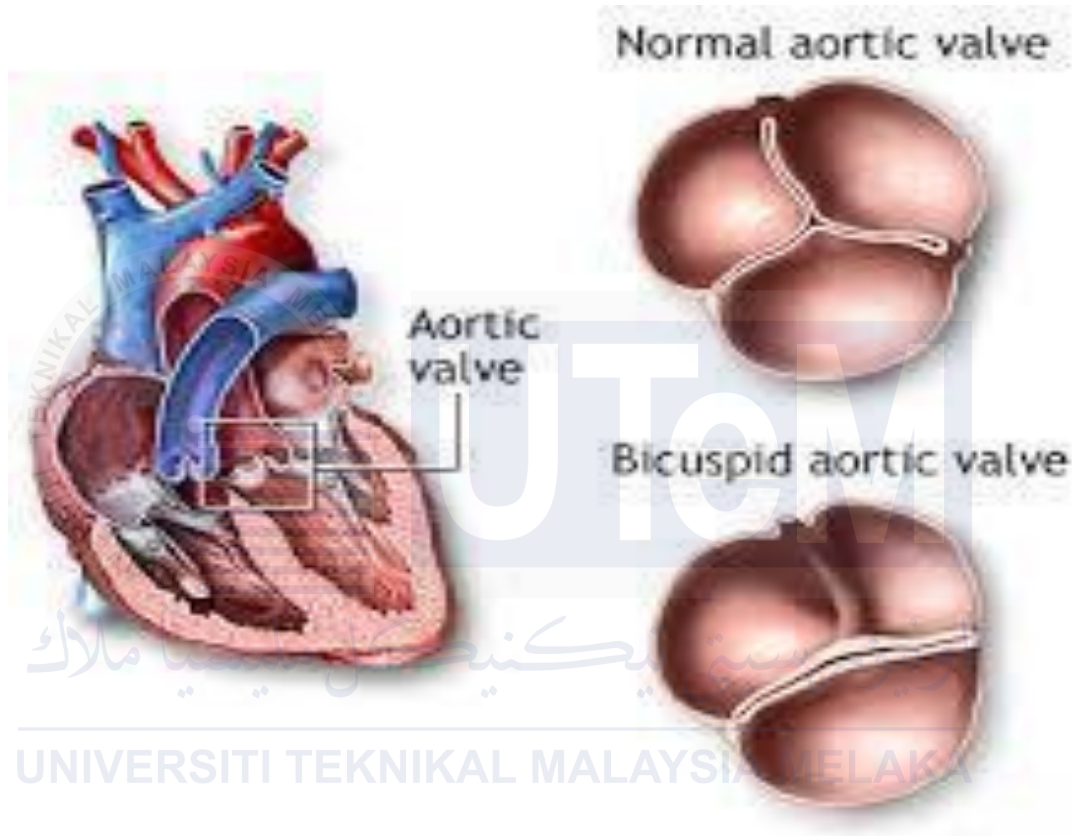


Figure 2.6 A diagram of a healthy compared to bicuspid aortic valve

In summary, numerous conditions can lead to aortic aneurysms, such as bicuspid aortic valve disease, penetrating atherosclerotic ulceration, Marfan syndrome, degenerative aortic aneurysms, pseudonyms, and thoracic aortic aneurysms. Degenerative aneurysms arise from the weakening and thinning of the aorta's muscular layer and connective tissue, which increases the risk of rupture or dissection (Sörelis et al., 2023). When cholesterol plaque builds up in the arteries, it can lead to penetrating atherosclerotic ulceration, which enlarges the arteries or creates holes in the aortic wall (Sörelis et al., 2023). Damage to the aortic wall that results in blood clots outside the wall causes pseudonyms.

2.1.3 Treatment for Aortic Aneurysms

To address this issue (Aortic Aneurysm) and lessen its impact on patients, several treatment approaches have been implemented globally. The first one is endovascular aneurysm repair (EVAR), which uses cardiac catheterization and is less invasive than open surgical repair. This is because the cut is smaller, and patients usually need less recovery time. EVAR is used to repair abdominal aortic aneurysms more often than thoracic aortic aneurysms. During the procedure, the patient's surgical team makes a small cut, usually in the groin, then guides a stent graft in a tube covered with fabric through the patient's blood vessels up to the aorta. The stent graft then expands and attaches to the aortic walls. A seal forms between the stent graft and the vessel wall to prevent blood from entering the aortic aneurysm.

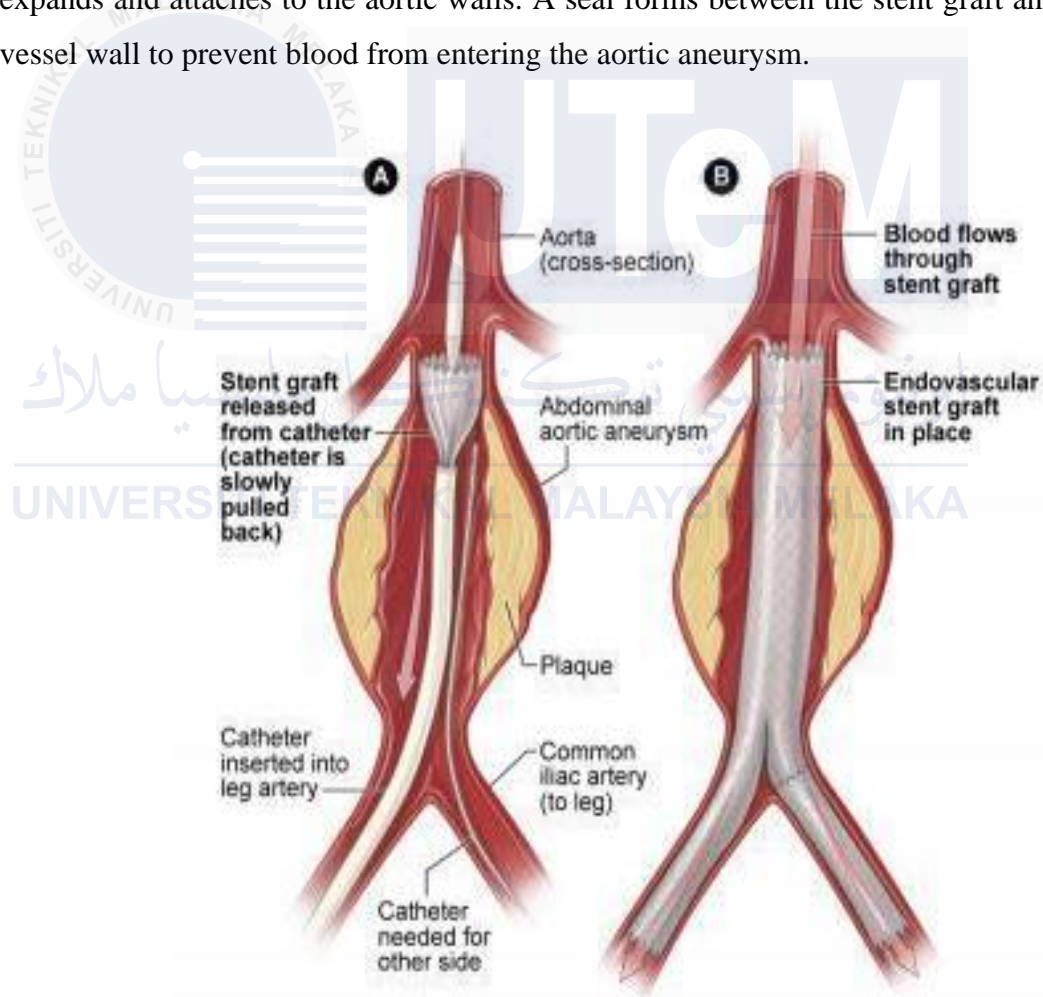


Figure 2.7 The illustration shows the placement of a stent graft in an abdominal aortic aneurysm. In figure A, a catheter is inserted into an artery in the groin. The catheter is threaded to the abdominal aorta, and the stent graft is released from the

catheter. In figure B, the stent graft is expanded and allows blood to flow through the aorta.

In summary, Endovascular aneurysm repair (EVAR) is a more conservative treatment method for aneurysms of the aorta, which are more common than thoracic aortic aneurysms. EVAR entails making a small cut in the groin and inserting a stent graft through the patient's blood vessels to the aorta. A seal forms between the stent graft and the vessel wall, preventing blood from entering the aneurysm. Open aneurysm surgery, also known as open surgery, aims to prevent rupture or dissection of an aneurysm while also repairing any damage. The damaged aorta section is removed and replaced with a synthetic fabric tube that acts as a new lining for the patient's artery. This major surgery necessitates a significant incision in the patient's abdomen or chest.

2.2 Cardiovascular Computed Tomography Angiography (CCTA)

A cardiac CT angiography (CCTA) scan is a non-invasive diagnostic procedure that utilises X-rays to generate precise visual representations of the heart and its associated blood vessels. A computer compiles these images to create a three-dimensional (3D) representation of the heart, which is used to assess the existence and severity of stenosis (narrowing) in the coronary arteries and blood vessels responsible for supplying blood to the heart and other organs (Cardiac Computed Tomography Angiography, 2023). Multidetector CT (MDCT) scans are rapid and intricate, yielding superior-quality images while minimising radiation exposure (Hagen et al., 2022).

CT scanners are essential medical devices used to analyse the anatomical structures of the body. The detectors they use include first-generation, second-generation, third generation, and fourth-generation models, which specifically absorb the low-energy portion of the X-ray spectrum (Hagen et al., 2022).

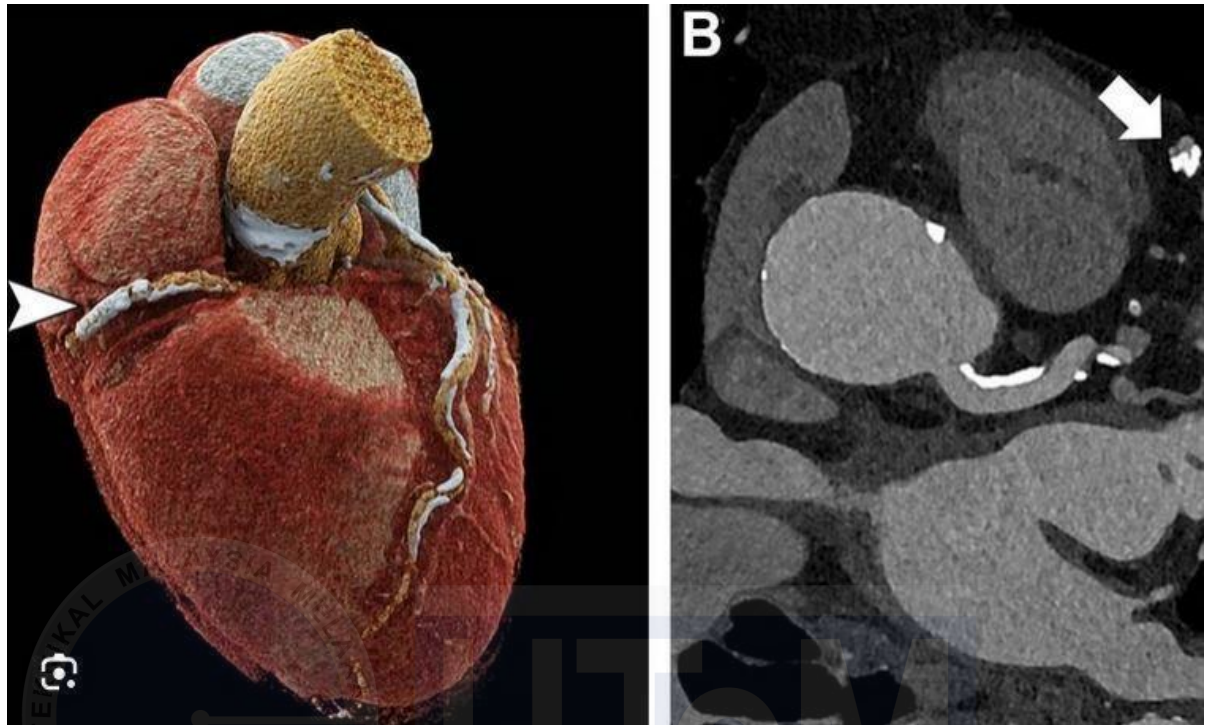


Figure 2.8 An example of Cardiac Computed Tomography Angiography (CCTA) or Cardiac CT scan

2.2.1 What is Computed Tomography (CT)?

The term “computed tomography,” or CT, refers to a computerised x-ray imaging procedure in which a narrow beam of x-rays is aimed at a patient and quickly rotated around the body, producing signals that the machine’s computer processes to generate cross-sectional images, or “slices” (Hagen et al., 2022). These slices, known as tomographic images, can provide clinicians with more detailed information than conventional x-rays. The machine’s computer can gather several consecutive slices, which can then be digitally “stacked” to create a three-dimensional (3D) image of the patient. This makes it simpler to identify the patient’s basic anatomy as well as any potential tumours or abnormalities (Hagen et al., 2022).



Figure 2.9 A computed tomography (CT) scan of a human heart rendered using (a) gradient-based diffuse shading, (b) our method using local visibility, and (c) our method using global visibility.

2.2.2 How does a CT scan work?

A CT imaging system transports a patient through a circular opening via a motorised table. The patient is exposed to a narrow, fan-shaped beam of x-rays that can be as small as 1 millimetre or as large as 10 millimetres (Hagen et al., 2022). The examination usually consists of several phases, each with 10 to 50 rotations of the x-ray tube around the patient. To visualise vascular structure, the patient may be given an injection of “contrast material” (Cardiac Computed Tomography Angiography, 2023).

Detectors on the patient’s exit side capture the x-rays as an x-ray “snapshot” from one position of the x-ray source. During a single complete rotation, many different “snapshots” are captured. The data is sent to a computer, which reconstructs all the individual “snapshots” into a cross-sectional image of the internal organs and tissues for each complete rotation of the x-ray source (Hagen et al., 2022).



Figure 2.10 Patient in CT Imaging System

2.2.3 What are the key components and principles of a CT scan?

CT scanners are vital medical instruments for examining the body's structures. A generator produces X-rays, which are subsequently transformed into X-ray photons through thermionic emission (Hagen et al., 2022). The X-ray tube, an essential element of CT, is a structure that contains the X-ray tube, shielding components, and photon detectors. The gantry tilt, ranging from -25 to +25 degrees, facilitates uninterrupted

circular motion of internal components while maintaining the organisation of circuits and cables (Hagen et al., 2022). The X-ray tube comprises a cathode assembly, an anode assembly, and a rotor, all contained within a tube envelope. Contemporary CT scanners generally possess an electrical power range of 20 to 60 kW.

The cathode filament generates electrons via thermionic emission, and elevated voltages further accelerate the emitted electrons. When electrons impact the anode's focal point, two forms of electromagnetic radiation are generated: characteristic and bremsstrahlung X-rays. The focal spot size can be adjusted to attain the requisite image resolution (Hagen et al., 2022). The photon detector, or photovoltaic cell, absorbs and quantifies photons emitted by X-ray tubes that traverse a patient. CT scanners employ multiple detector types, comprising first-generation, second-generation, third generation, and fourth-generation models (Hagen et al., 2022). Collimators are substances that attenuate the low-energy segment of the X-ray spectrum.

They protect individuals in proximity during the scan and diminish scattered radiation, consequently reducing image noise (Hagen et al., 2022). CT machines are equipped with collimators, including source and detector collimators. The diaphragm configures the X-rays generated by the X-ray tube into a beam shape, while the grid absorbs numerous photons that stray from their designated trajectory prior to impacting offline detectors. Table pitch, also known as detector pitch, refers to the distance of the patient's gantry rotation. Elevated pitches decrease scanning duration and radiation exposure; however, they may also diminish image resolution if the machine's circuitry is incapable of processing information as swiftly as the table. (Hagen et al., 2022).

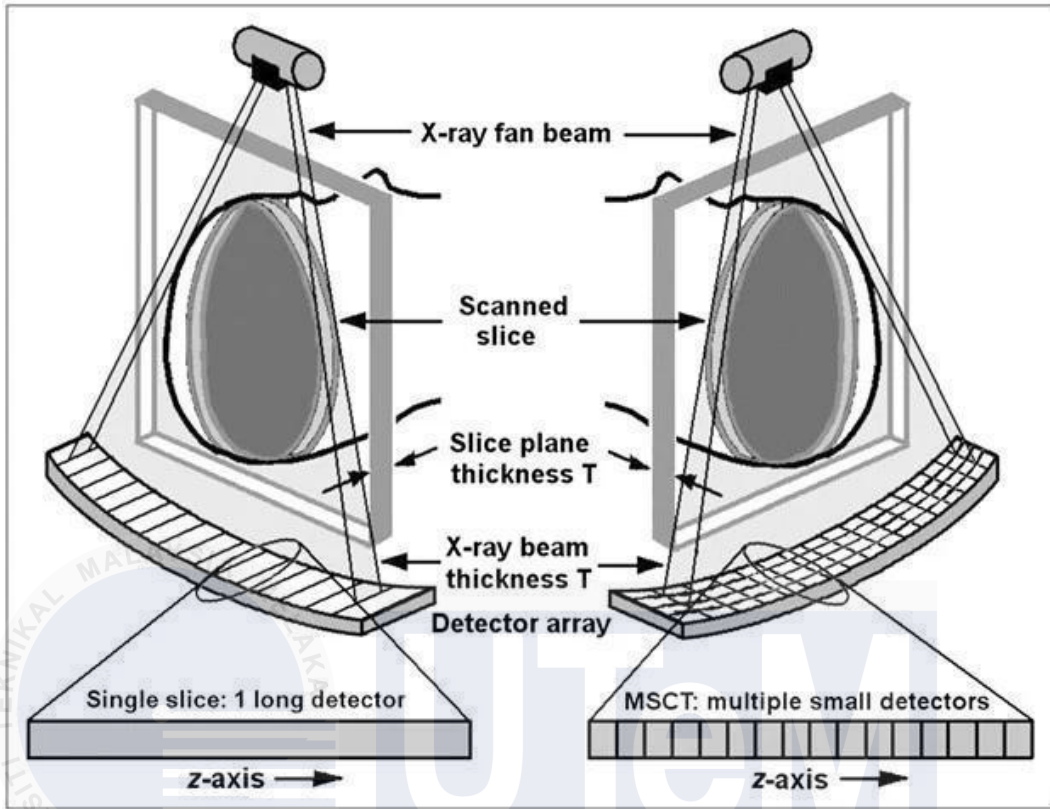


Figure 2.11 Slice of CT Scanner



Figure 2.12 CT Scanner



Figure 2.13 CT Scanner Control Room

2.2.3.1 Generator

The generator supplies the necessary electrical power to produce x-rays by utilising two distinct forms of electrical current. A high voltage supply that ranges from 20 to 150 kilovolts determines the maximum intensity of X-rays produced (Hagen et al., 2022). Raising the voltage amplifies the electrical potential difference between the anode and cathode. A low voltage that stays the same (about 10 kilovolts) is applied to the cathode filament. This lets electrons flow continuously through a thermionic reaction (Hagen et al., 2022).

2.2.3.2 Formulas

A scanning unit, commonly referred to as a gantry, is a framework that houses the X-ray tube, shielding components, and photon detectors (Hagen et al., 2022). The X-ray tube and photon detectors are aligned in a face-to-face position and designed to rotate 360 degrees in a single direction around the patient. The gantry tilt refers to the angle between the plane of the X-ray tube and the vertical plane. In most modern machines, the gantry

tilt can vary from -25 degrees to +25 degrees (Hagen et al., 2022). The CT operator can change the gantry tilt based on the exam objectives, such as reducing image artefacts or improving a healthcare provider's ability to perform an invasive CT-guided procedure. The use of slip rings in gantries allows for continuous, complete circular movements of the internal elements while keeping the internal circuits and cables untangled. The gantry includes a passage for the table and the patient to traverse. The initial availability of CT was limited to imaging of the head. However, in 1976, a larger gantry was created, enabling the scanning of the entire body (Hagen et al., 2022).

2.2.3.3 X-ray Tube

The X-ray tube converts the kinetic energy of electrons (i.e., electricity) into X-ray photons, which exhibit distinct energetic properties such as wavelength and amplitude (Hagen et al., 2022). The X-ray tube comprises a cathode assembly, an anode assembly, and a rotor, all encased within a tube envelope, collectively referred to as the tube insert. The interior of the tube envelope has been entirely devoid of all gas atoms, resulting in the formation of a vacuum. Modern CT scanner X-ray tubes generally possess an electrical power range of 20–60 kilowatts (Hagen et al., 2022).

The cathode filament releases electrons through thermionic emission, wherein the current from the X-ray generator vaporises electrons. The voltage differential between the cathode and anode propels the emitted electrons, with increased voltages further enhancing their acceleration. Two types of electromagnetic radiation are emitted when electrons strike the anode's focal point.

The first type is characteristic X-rays, emitted when an accelerated free electron collides with the nucleus of a target atom, resulting in the ejection of one of the atom's inner shell electrons. The second type is braking X-rays, emitted when an accelerated free electron traverses the target atom and dissipates kinetic energy (Hagen et al., 2022). The focal spot size can be modified to attain the desired image resolution; smaller focal sizes yield higher image resolution. The procedure transforms electric energy into 99% thermal energy and merely 1% photons, while oil is retained between the tube envelope and tube housing for the purposes of equipment cooling and insulation (Hagen et al., 2022).

2.2.3.4 Detectors

The photon detector, also called a photovoltaic cell, absorbs, and counts photons emitted by X-ray tubes passing through a patient (Hagen et al., 2022). It is composed of two layers: the scintillator layer and the photon tide layer. The first-generation CT scanners had two detectors, allowing for two simultaneous views. Second-generation scanners featured 30 detectors arranged in a single row, covering a 10-degree fan angle. Third-generation scanners included up to 900 multi-row detectors, allowing for simultaneous scanning of multiple tissue slices, reducing scan time, improving resolution, and increasing X-ray tube power efficiency. Fourth-generation scanners use up to 4500 stationary detectors arranged in a circle around the patient (Hagen et al., 2022).

2.2.3.5 X-ray Shielding Elements

X-rays that do not travel in a straight path from the X-ray tube to the detector in line with the beam but instead end up at an off-path detector interfere with the machine's ability to reconstruct an accurate representation of what signal was derived from what original location (Hagen et al., 2022). This phenomenon, along with other types of image processing inaccuracies, causes image "noise," which reduces the contrast between imaged structures, which is critical for maintaining image quality and allowing for interpretation of anatomy and pathology (Hagen et al., 2022).

CT machines, like other types of X-ray imaging equipment, include collimators, which are materials that can absorb the low-energy portion of the X-ray spectrum (Hagen et al., 2022). These materials shield (i.e., reduce the overall X-ray exposure of) people nearby during the scan while also reducing scattered radiation, which reduces image noise. CT scanners have two types of collimators: source collimators (also known as diaphragms) and detector collimators (also known as grids). The diaphragm directs the X-rays produced by the X-ray tube into a beam shape. Despite the formation of a highly focused beam, as the X-ray photons pass through the patient, the atoms deflect and scatter the photons in all directions. The grid absorbs many of the photons that deviate from their intended path before they strike offline detectors and can be submitted for image processing, where they interfere with the measurements obtained from the inline photon beams. The grid also reduces the number of photons required for image production, indirectly lowering the patient's overall radiation exposure (Hagen et al., 2022).

2.2.3.6 Patient Table

The patient's table moves through the gantry during the scan. The table pitch, also known as the detector pitch, is the distance the table moves during a complete gantry rotation (Hagen et al., 2022). Table pitch is the ratio of beam collimation (slice thickness in mm) to the forward table movement in millimetres (mm) during a full gantry rotation. Faster-moving tables are described as having higher pitches. Increased table speed reduces scanning time and radiation, but it can also reduce image resolution if the machine's circuitry is unable to process information as quickly as the table (Hagen et al., 2022).

2.2.4 Certification for Cardiovascular Computed Tomography (CCT)

Several training statements made by the British Society of Cardiovascular Imaging and the Royal College of Radiologists include cardiovascular computed tomography (CCT) training. These include the Royal College of Radiology's Clinical Radiology Specialty Training Curriculum 2020, the CCT Core Syllabus of the European Association of Cardiovascular Imaging, and the 2014 Royal College of Radiologists/British Society of Cardiovascular Imaging document (Cardiac Computed Tomography Angiography (CCTA), 2023). The Society of Cardiovascular Computed Tomography (SCCT) also released a comprehensive curriculum for program directors in radiology and cardiology (Bertolini, Rossoni, & Colombo, 2021). The purpose of this document is to offer programme directors guidance on creating a curriculum for the training of independent practitioners (IPs) and/or advanced practitioners (APs) (Chen, Fernandez, Xu, Velliou, Homer-Vanniasinkam, & Tiwari, 2023). The Accreditation Council for Graduate Medical Education (ACGME) in the United States adopted six fundamental competencies for trainee education and evaluation (Ludvigsen, Nagaraja, & Daly, 2021).

Table 2.1 Summary of Independent Practitioner (IP) and Advanced Practitioner (AP) capabilities upon completion of training.

Final Training Level	Definition
----------------------	------------

Independent Practitioner (IP)

- Achieved competency to independently interpret cardiac findings on non-contrast and contrast-enhanced cardiac CT
- Achieved competency to independently evaluate patient selection, preparation, scan protocol selection, dose modulation, post-processing, and image interpretation
- Expertise in all common cardiac CT tasks, such as figuring out what is wrong with the coronaries and how they work, as well as basic structural HD assessment, EP procedural planning, basic congenital HD, and functional CT.



اونيورسيتي تيكنيكل مليسيا ملاك

UNIVERSITI TEKNIKAL MALAYSIA MELAKA

Advanced Practitioner (AP)

- Achieved competency in all capabilities ascribed to the IP level of training.
- Achieved advanced skills and knowledge beyond IP, including evaluation of complex coronary artery disease, competency in structural heart planning and a wider spectrum of congenital heart disease
- Achieved competency in vascular CT
- Achieved competency in laboratory accreditation requirements and maintenance
- Achieved competency in equipment purchasing, maintenance, and acquisition
- Actively involved in quality improvement, performance improvement, and/or CT-specific research endeavours
- Achieved competency in business aspects (billing, coverage, reimbursement, and prior authorization) of CT laboratory administration

Cardiovascular Computed Tomography (CCT) is growing rapidly, so courses of study must adopt a comprehensive curriculum to meet the growing need for independent practitioners (IP) and advanced practitioners (AP) with a minimum of experience and a core understanding of all CCT aspects (Bertolini, Rossoni, & Colombo, 2021). The curriculum should include multispecialty lectures, webinars, societal education, and annual scientific meetings. In smaller courses, online training, webinars, and simulations may be useful (Chen, Fernandez, Xu, Velliou, Homer-Vanniasinkam, & Tiwari, 2023). Advanced practitioner training should emphasize complex CCT applications, complex cardiac disease, multidisciplinary collaboration, and cardiology and radiology skills. Direct mentoring from the lab director or other AP supervisors is critical (Ludvigsen, Nagaraja, & Daly, 2021).

In summary, the British Society of Cardiovascular Imaging and the Royal College of Radiologists have issued guidelines for cardiovascular computed tomography (CCT) training. These include the Clinical Radiology Specialty Training Curriculum 2020, the European Association of Cardiovascular Imaging's CCT Core Syllabus, and the Royal College of Radiologists/British Society of Cardiovascular Imaging document from 2014 (Cardiac Computed Tomography Angiography (CCTA), 2023). The Society of Cardiovascular Computed Tomography (SCCT) has developed a comprehensive curriculum for programme directors in radiology and cardiology (Chen, Fernandez, Xu, Velliou, Homer-Vanniasinkam, & Tiwari, 2023). The Accreditation Council for Graduate Medical Education (ACGME) has established six core competencies for trainee education and evaluation (Ludvigsen, Nagaraja, & Daly, 2021).

2.3 Three-dimensional (3D) Printed Model

Chuck Hull created the first 3D printer in 1987 after Hideo Kodama pioneered the development of the initial 3D printing production equipment in 1981 (how does 3d printing work - Google Search, n.d.). In the 1990s, there was an expansion in the industry, culminating in the commercial availability of the first selective laser sintering (SLS) printer in 2006 (Teaching Tech, 2020). The RepRap Project transformed the field of 3D printing by reevaluating additive manufacturing techniques, specifically FDM and FFF, resulting in the development of affordable 3D printers (Muskan, Gupta, & Negi, 2022).

The success of RepRap expedited the emergence of commercial 3D printers, enticing manufacturers such as Makerbot and Thingiverse (PRECISE3DM, 2021).

The data from the CT scan is transformed into computer-aided design (CAD) models to accurately align the geometry with the desired design (Hagen et al., 2022). This procedure entails obtaining precise CT 3D images, which may be analysed using 3D inspection instruments and reverse engineering software (Mørup, Stowe, Precht, Gervig, & Foley, 2022). The data is commonly found in STL format and can be transformed into a compatible file format (Capelli, Bertolini, & Schievano, 2023). PrinterPrezz utilises Synopsys' Simpleware ScanIP software to analyse and segment MRI and CT scan data, rebuilding it in a sequential manner (Mahajan et al., 2020). The 3D model is subsequently produced using resin, guaranteeing adherence to the original design (Geng et al., 2023).

2.3.1 The Origin of 3D Printing Techniques

Hideo Kodama indeed invented the first 3D printing manufacturing equipment in 1981, drawing on Ralf Baker's work from the 1920s (how does 3d printing work - Google Search, n.d.). His work in laser-cured resin rapid prototyping expanded over the next three decades with the introduction of stereolithography in 1984 (Marconi, Alaimo, & Mauri, 2022). Chuck Hull of 3D Systems invented the first 3D printer in 1987, which used stereolithography (Teaching Tech, 2020). Other 3D printing systems were created in the 1990s and 2000s, but their costs fell substantially once patents expired in 2009, making the technology available to a wider range of customers (Muskan, Gupta, & Negi, 2022).

Chuck Hull invented stereolithography in 1983 and established 3D Systems to produce and sell a commercial printer (Cardiac Computed Tomography Angiography (CCTA), 2023). Currently, Hull's design for 3D printers is extensively employed for manufacturing intricate parts using a diverse range of materials (Capelli, Bertolini, & Schievano, 2023).



Figure 2.14 SLA-1, the first commercial prototyping device from 3D Systems

The RepRap project, which was open-source and made 3D printing technology available to anybody with a computer, was chosen the most significant 3D printed item by 3Dprint.com in 2017 (Branzan et al., 2021). The success of RepRap accelerated the rise of commercial 3D printers, with many patents filed in the 1980s entering the public domain in 2006. This resulted in a rush of 3D printing manufacturers, including Makerbot, which introduced 3D printing to the public market and opened opportunities for both professional and amateur users. Makerbot marketed open-source DIY kits, and its online file repository, Thingiverse, hosted hundreds of thousands of free and paid 3D printing files, making it the largest online 3D printing community (Hagen et al., 2022).



Figure 2.15 The machine on the left produced all the plastic parts for the machine on the right. Adrian Bowyer (left) and Vik Olliver (right) are members of the RepRap project.

Since the introduction of commercial 3D printers, the landscape of the industry has evolved dramatically. In addition to the aerospace industry, architecture, manufacturing, automotive, healthcare, and construction, 3D printers are also being utilised in a wide range of other businesses and sectors.

2.3.2 What is 3D Printing? How does it work?

Three-dimensional (3D) printing is an additive manufacturing technique that produces a physical product from a digital design (Marconi, Alaimo, & Mauri, 2022). The technique operates by depositing thin layers of material, such as liquid or powdered plastic, metal, or cement, and subsequently bonding the layers together (how does 3d printing work - Google Search, n.d.).

Medical 3D printing is a process that converts 2D images into a 3D surface model composed of triangles, producing a file format called STL (Muskan, Gupta, & Negi, 2022). The procedure entails utilising imaging techniques such as CT, MRI, and ultrasound to guarantee accurate calibration. The 2D photos are subsequently converted into a triangulated 3D surface model using specialised software and user involvement. During the initial phase in dentistry, a 3D scanner is utilised to transform anatomical structures into digital 3D models. If the desired product is not an anatomical model, the 3D surface model is generated using various CAD tools. Automated methodologies such as finite-element analysis and parametric design can be employed to improve or adapt designs to accommodate many patients.

During the third phase, the 3D surface models are transformed into layers and commands, which are commonly referred to as G-code. The G-code commands serve as instructions to the printer, directing it to create physical objects using the printing procedure. Designers have the option to either provide parameters or choose the material for the printer operator. The printer operator or end user is responsible for doing post-processing procedures, such as washing, polishing, and sterilisation, to achieve the

desired surface quality. The last phase entails the actual execution of the product by the clinician who made the printing request.



2.3.2.1 CT scan to 3D CAD Design

Conversion of CT scan data into a computer-aided design (CAD) model is a crucial process in many industries, particularly in healthcare and manufacturing. By utilizing a CT scanner, highly precise 3D images can be obtained, providing accurate internal and external surface geometry (Hagen et al., 2022). This data can be accurately analyze using 3D inspection tools and replicated in reverse engineering software (Mørup, Stowe, Precht, Gervig, & Foley, 2022).

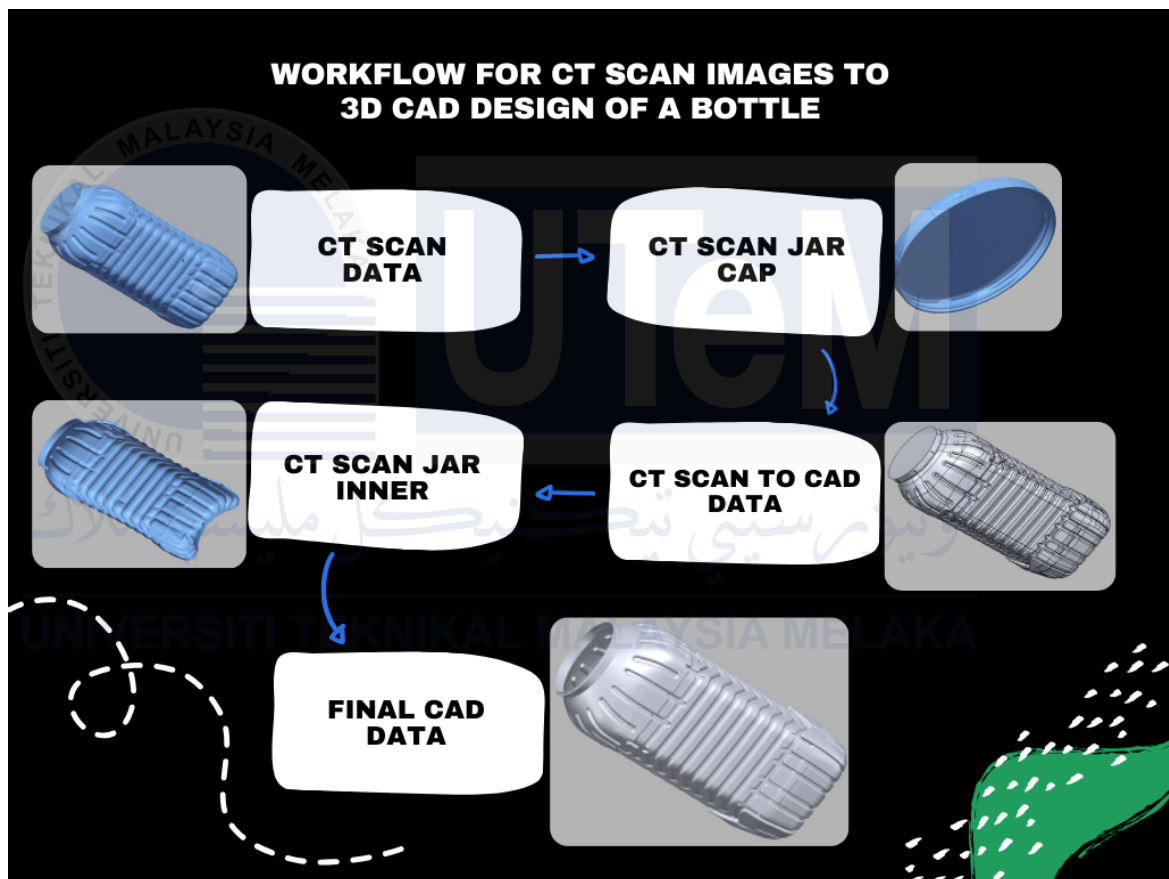


Figure 2.16 An example of a workflow for CT Scan images to 3D CAD Design of a bottle/jar

Another example of the application of 3D printing in the medical field is the processes used at PrinterPrezz, which include converting MRI and CT scans into 3D CAD images for 3D printing (Branzan et al., 2021). Precision imaging, measurements, and design are used in this procedure to produce medical devices that are specific to everyone's anatomy (Capelli, Bertolini, & Schievano, 2023). The team employs Synopsys' Simpleware ScanIP to analyse and segment MRI and CT scan data, enabling

for layer-by-layer reconstruction (Mahajan et al., 2020). This procedure separates bone structures from other bodily parts, including organs and muscles (Geng et al., 2023). After developing a 3D model, it is printed in resin to give a physical replica of the MRI or CT scan (Muskan, Gupta, & Negi, 2022). The team then uses MRI and CT scans to study the 3D printed parts inside structure, indicating potential structural and design improvements (Hagen et al., 2022). This technique ensures that the 3D printed part is consistent with the original design from the start (Mørup, Stowe, Precht, Gervig, & Foley, 2022).



Figure 2.17 A CT scan of a Spine, made up of many 2D “slices”



Figure 2.18 3D Printed Model of a spine section

2.3.2.2 General workflow in making 3D-Printed Model

3D printing is a breakthrough method that enables the development of digital models of objects that can be produced using a 3D printer. There are four stages involved in this process: modelling, slicing, printing, and post-processing in the end.

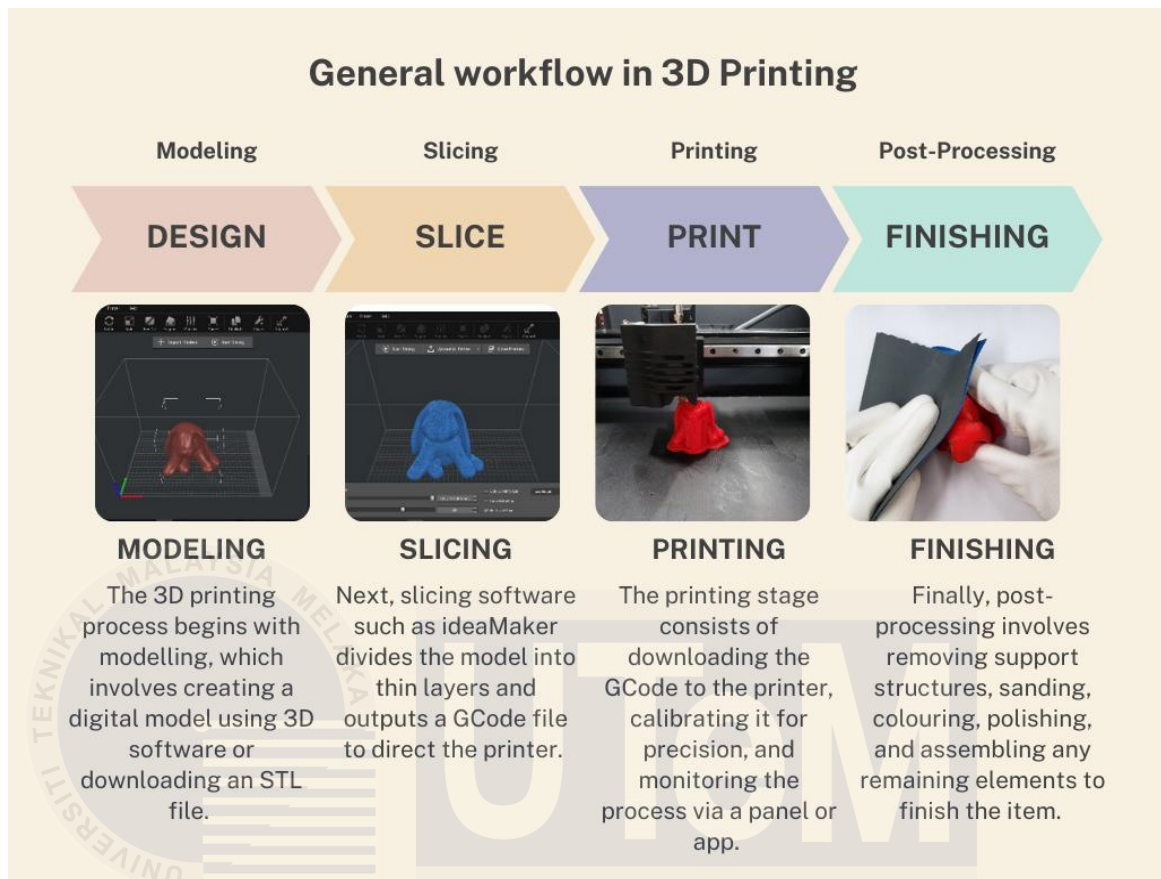


Figure 2.19 shows a general workflow in 3D printing

Constructing a digital model of the thing is an essential part of the modelling process. This model can be made with the help of 3D modelling software or downloaded from other users. STL files are commonly used for rapid prototyping, 3D printing, and computer-aided manufacturing (CAM). Raise3D's IdeaMaker Library provides a platform for sharing and obtaining 3D modelling models and configuration files (PRECISE3DM, 2021). Using specialised slicing software such as IdeaMaker, the model is cut into slices, which enables the 3D printer to determine the path and the amount of filament that will be needed for printing. This method allows the printer to create a GCode file, which is effectively a long set of instructions that the 3D printer uses to make the model (PRECISE3DM, 2021). After the slice file has been sliced, it is then uploaded to the printer and calibrated to get it ready for printing. The extruders and printing base must be calibrated to improve printing accuracy. It is possible to see the printing process through the transparent panel of a Raise3D Pro2 Series printer or to remotely monitor the progress through the RaiseCloud app in real time. Both options are available during the printing process (PRECISE3DM, 2021). Post-processing is the final stage of the 3D printing process, which begins with

the removal of support and continues with sanding, colouring, polishing, and polishing. When printing a multi-part or huge model, it is feasible to separate the parts and join them to produce a complete model (PRECISE3DM, 2021).

2.3.2.3 Medical 3D Printing Process

To comprehend the legal concerns surrounding medical 3D Printing, it is imperative to have a thorough understanding of the procedure itself (Bicudo, Faulkner, & Li, 2020). Although our current discussion focuses on 3D printing, the methods we are about to describe are applicable to any patient-matched medical equipment, regardless of the manufacturing technology (Bicudo, Faulkner, & Li, 2020). The radiology department usually obtains imaging data, such as CT, MRI, and ultrasound, to ensure precise calibration. Consequently, a sequence of 2D images in grayscale is generated and stored in a DICOM file, which includes confidential patient data (Song, Du, Zhang, & Li, 2022). The process of imaging for 3D printing has specific prerequisites that must be considered from the outset to generate an ideal model (Song, Du, Zhang, & Li, 2022).

The printer operator or end user may undertake post-processing tasks, such as washing, polishing, and sterilisation, based on the desired surface quality. The ultimate stage involves the practical implementation of the product, usually by the clinician who

requested

the

print.

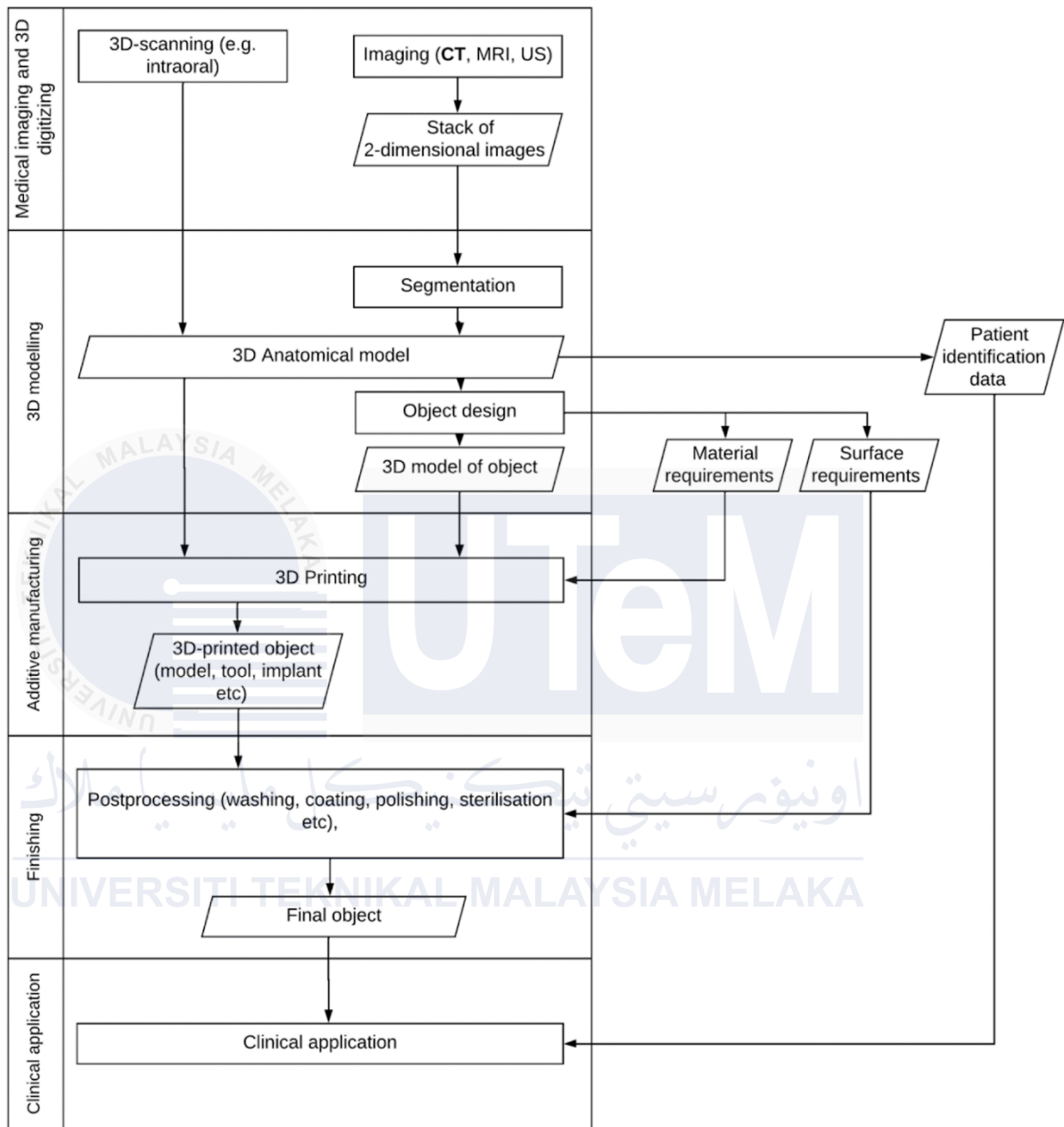


Figure 2.20 A process description of clinical 3D printing. Parallelograms serve as symbols for real-world objects, software, documents, and data, while rectangles serve as descriptions of various process steps. Each of these steps contributes to the final quality of the product. A 5-step classification of the various processes is presented on the left.

The picture illustrates how the 3D printing process enables a decentralised production network. Occasionally, the designer may also serve as the surgeon, and the printing is done within the hospital. However, in other cases, the manufacturing or design

may be contracted out to a service provider, who may then subcontract certain types of printing, like metallic additive manufacturing, to other companies.

2.4 Acts & Legislation in Medical 3D-Printed Models

The Medical Device Regulation (MDR) of the European Union regulates the pre-market control of medical devices, which includes software used in 3D printing toolchains (Ludvigsen, Nagaraja, & Daly, 2021). The proposed modification of the EU Product Liability Directive seeks to broaden the scope of the 1985 Product Responsibility Directive and tackle issues related to defects and compensations in the digital age (Daly, 2023). The Directive aims to address any defects in products at any point in the custody chain, including service providers and equipment providers (Bicudo, Faulkner, & Li, 2020). The 'Learned Intermediary Doctrine' enables manufacturers to relieve themselves of the need to educate patients of potential dangers by relying on healthcare practitioners' duty to provide such information (Daly, 2023). 3D printing is subject to intellectual property rights, which encompass copyright, patent, trademark, and design rights (Bicudo, Faulkner, & Li, 2020).

3D printing enables the creation of customised medical items by utilising imaging data in a decentralised and immediate manner (Marconi, Alaimo, & Mauri, 2022). Nevertheless, the occurrence of medical procedures at healthcare facilities raises additional inquiries regarding the implementation of regulations pertaining to medical devices in such scenarios. The CDRH is creating a structure to govern 3DPOC devices used in different production environments. The agency has organised webinars in partnership with the American Society of Mechanical Engineers (ASME) to collect feedback on its previous five-scenario framework. As the use of 3DPOC becomes more widespread, medical organisations and professional bodies may establish their own guidelines, similar as the Radiological Society of North America's 2018 Guidelines for 3D-printed anatomical models (Daly, 2023).

2.4.1 European Union (EU)

The Medical Device Regulation (MDR) in the European Union (EU) is a regulatory framework that oversees the pre-market regulation of medical devices,

considering their risk classifications (Ludvigsen, Nagaraja, & Daly, 2021). Band-aids are classified as Class I medical devices, whereas life-supporting items are classified as Class III medical devices. The recently implemented Medical Device Regulation (MDR), which came into effect in May 2021, focuses on the categorization of products and the procedures for obtaining market authorization. The software utilised in 3D printing toolchains may meet the criteria for being classified as “Software as a medical device,” and hence be subject to safety and performance regulations (Ludvigsen, Nagaraja, & Daly, 2021). The MDR also governs devices that are “mass customised,” with a Custom Device Exemption that exempts devices created according to a written description from some criteria, such as acquiring CE-marking. Nevertheless, this exception does not absolve a product from most standards, including the necessity of maintaining a quality management system. The EU MDR governs both devices that are sold on the market and those that are produced and utilised within healthcare facilities, which are “put into service” (Ludvigsen, Nagaraja, & Daly, 2021).

Intellectual property (IP) law encourages inventive endeavours by granting producers of artistic works or inventors of technical advancements exclusive, transitory, and restricted rights (Bicudo, Faulkner, & Li, 2020). Intellectual Property Rights (IPR) encompass copyright, patent, trademark, and design rights, all of which are applicable to 3D printing (3DP). Copyright protection safeguards unique works of intellectual effort, patents confer rights on novel technical inventions, trademarks shield distinguishing signs, and design rights safeguard the visual appearance of products. Intellectual property rights encompass the authority to prevent others from utilising certain subject matter, including copyright, patent, and protected signs (Bicudo, Faulkner, & Li, 2020).

Table 2.2 IPR types, subject matter, and purpose.

Type	Subject Matter and Purpose
Copyright	Right related to original/creative works, including literary, theatrics, musical, and other artistic works (including software); right is only against copying and lies in the expression of an idea rather than its general concept or character. In the EU, copyright attaches

	<p>automatically to the creation with no need for registration and lasts for 70 years after the death of the author.</p>
<p>Patents</p>	<p>A negative exclusionary right that can be obtained for technical inventions that are novel, involve an inventive step, are industrially applicable, and sufficiently disclosed. Patent Holders are allowed to exclude others from practising the invention in exchange for public disclosure of the invention (quid pro quo). Patents are granted after a formal examination process, and they last for 20 years after the filing date.</p>
<p>Trademark</p>	<p>Right to exclusive use of any sign (e.g., words, letters, numerals, pictures, shapes, colours, sounds, smells, etc.) by which consumers can identify the source of goods or services. In the EU, trademarks should be registered through a formal examination process; they can last indefinitely if they are renewed.</p>
<p>Industrial designs</p>	<p>Right to the original, ornamental, and non-functional feature (i.e., the appearance) of the whole or part of an industrial or handcrafted product resulting from the features in the lines, contours, colours, shape, texture, and/or materials used. In the EU, designs can be registered through a formal examination process (registered design) or arise automatically without registration (unregistered design). They last up to 25 years.</p>

The European Union has made numerous efforts to standardise the various aspects of intellectual property rights (IPR) within its system (Bicudo, Faulkner, & Li, 2020). As a result, there is a substantial body of EU Directives and Regulations, along with several legal interpretations by the Court of Justice of the European Union (CJEU) (Bicudo, Faulkner, & Li, 2020). However, national legislation and legal precedents are equally significant and applicable, with many aspects of intellectual property rights still reflecting a distinct national character (Bicudo, Faulkner, & Li, 2020).

The GDPR includes a broad restriction on processing personal data, although there are exceptions for cases where data subjects have given their consent. This consent is usually acquired through a positive action and encompasses all activities pertaining to the processing of data for the same objective. Special safeguards are provided for biometric and health data; however, the classification of 3D models as biometric or health data necessitates specific authorization from the individual whose data is being collected. Nevertheless, the requirement of professional confidentiality according to the laws of EU Member States can vary across different countries, and the criteria for compliance can also vary between different countries (Ludvigsen, Nagaraja, & Daly, 2021).

2.4.2 United States Food & Drug Administration

The FDA, a prominent regulatory body in the field of medical technology, has been employing 3D printing technology since the early 2000s to fabricate implants, surgical equipment, medications, cells, and tissues. This method enables the fabrication of intricate internal geometries in devices, such as spinal implants, which include a porous structure that promotes tissue growth and integration (Chen et al., 2023).

3D printing stands out from other technologies because it enables the production of medical goods customised to specific patients using their imaging data in a decentralised and on-demand manner. Additionally, it enables providers to create prototypes of medical items (Marconi, Alaimo, & Mauri, 2022). However, since the process takes place in new environments (specifically, within healthcare facilities instead of large-scale manufacturing plants that typically produce enormous quantities of identical products), there are further inquiries regarding the application of medical device regulations in these situations (Daly, 2023). CDRH is currently developing a framework to regulate 3DPOC devices. This framework is being developed for various production scenarios (Daly, 2023).

Table 2.3 Earlier Version of FDA’s Framework Included 5

Manufacturing Scenarios for 3DPOC

Scenario	Description
A	Minimal-risk 3D printing by a health care professional

B	Device designed by manufacturer using validated process: turnkey system
C	Device created by the manufacturer using a verified procedure: Enhanced prerequisites for healthcare professionals
D	manufacturer is co-located at the point of care
E	health care facility becomes a manufacturer

Table 2.4 Updated Version of FDA's Framework Now Consists of 3 Scenarios for 3DPOC

Scenario	Description	The entity responsible for designing or developing the device	Entity using the 3D printing system to produce devices	Entity responsible for complying with applicable regulatory requirements
1	A medical device manufacturing system (MDPS) is utilised in a health care facility.	Conventional manufacturing	Medical institution	Conventional manufacturing

2	Traditional manufacturer co-located at or near the health care facility site	Conventional manufacturing	Conventional producer, encompassing any subcontractor	Conventional producer, encompassing any subcontractor
3	A health care facility that takes on all the conventional obligations of a manufacturer.	Medical institution	Medical institution	Medical institution

3D printing in hospitals has increased over the last decade, with an emphasis on personalised medicine. However, the cost of 3D printing might be prohibitively expensive for many hospitals, as most insurance companies do not reimburse the usage of the technology. This costly commitment may limit widespread adoption. Professional medical associations are working to develop payment standards for 3D-printed products by gathering case data demonstrating improved patient outcomes. The American College of Radiology (ACR) and the American Medical Association (AMA) adopted Category III Current Procedural Terminology (CPT) codes for 3D-printed anatomical models and guides in July 2019. Permanent Category I codes, which most insurance companies typically reimburse, might eventually result from this information. ACR has also collaborated with the RSNA to establish the RSNA-ACR 3D Printing Registry, which collects case information from healthcare practitioners via point-of-care image-based anatomical models and surgical guidance (Marconi, Alaimo, & Mauri, 2022).

2.5 Summary or Research Gap

The existing literature indicates that the application of 3D printing and Cardiovascular Computed Tomography (CCT) in medical contexts signifies significant advancements capable of improving patient outcomes and diagnostic precision (Bertolini, Rossoni, & Colombo, 2021). To enhance the precision and personalisation of medical treatments, 3D-printed anatomical models should be utilised for surgical planning and CCT diagnosis of cardiac conditions (Branzan et al., 2021). The extensive implementation of these technologies is hindered by significant challenges, primarily due to their prohibitive costs and the lack of standardised training programs (Bicudo, Faulkner, & Li, 2020). No universally accepted protocol exists for integrating these technologies into clinical practice, despite numerous studies demonstrating their benefits (Capelli, Bertolini, & Schievano, 2023). Divergences and inconsistencies in the methodologies employed by healthcare professionals lead to variations in patient treatment and outcomes (Cardiac Computed Tomography Angiography (CCTA), 2023). Healthcare practitioners aim to deliver cost-effective, practical, and standardised approaches that ensure widespread applicability, high precision, and enhanced patient care (Chen, Fernandez, Xu, Velliou, Homer-Vanniasinkam, & Tiwari, 2023). These challenges have hindered the development of a universally accepted methodology for the broad implementation of CCT and 3D printing in medical practice (Daly, 2023).

Current literature suggests that while 3D printing has been extensively examined for its capacity to create accurate anatomical models, there is scant evidence regarding its long-term benefits and cost-effectiveness in clinical practice, especially across diverse healthcare settings (Geng et al., 2023). The comprehensive incorporation of 3D printing and CCT into conventional clinical protocols has not been adequately examined in any research (Göçer et al., 2021). Moreover, most studies have focused on the isolated applications of these technologies instead of developing a cohesive strategy that amalgamates 3D printing and CCT for enhanced therapeutic and diagnostic outcomes (Hagen et al., 2022).

Furthermore, while 3D-printed models possess significant potential for surgical planning and education, their impact on long-term patient outcomes and cost-effectiveness remains inadequately explored in the existing literature (Ludvigsen, Nagaraja, & Daly, 2021). Additionally, standardised training programs for medical professionals are

implemented to optimise the utilisation of advanced technology (Mahajan et al., 2020). The objective of this thesis is to establish a comprehensive, standardised protocol for the economical, precise, and improved patient outcomes integration of CCT and 3D printing into clinical practice (Marconi, Alaimo, Mauri, Negrello, & Auricchio, 2022). This study aims to address these gaps, facilitating the broader adoption and optimisation of innovative medical technology, ultimately enhancing patient care (Mørup, Stowe, Kusk, Precht, & Foley, 2022).

To address the challenges, there exists a research opportunity to explore and develop innovative, integrated, and effective methodologies for the implementation of CCT and 3D printing in clinical practice (Mørup, Stowe, Precht, Gervig, & Foley, 2022). This study aims to create cost-effective solutions and standardised training programs to facilitate the widespread adoption of these technologies in various healthcare settings (Mubarik, Sharma, & Law, 2023). Chapter 3 will provide an in-depth examination of the proposed methods.

CHAPTER 3

METHODOLOGY

3.1 Introduction

This chapter defines a detailed process for producing patient-specific 3D printed models of Aortic Artery Aneurysms (AAA) utilizing CT scan pictures. The process consists of five principal stages: Image Acquisition, Image Segmentation, 3D Reconstruction, 3D Printing, and CFD Simulation. Each phase is essential to the overall process and has been carefully crafted to ensure the creation of accurate and dependable 3D models.

The Image Acquisition step requires procuring high-resolution spiral CT angiography images of the patient's aorta. This process guarantees that the obtained images possess adequate quality to precisely depict the details of the aorta and the aneurysm. The Image Segmentation phase employs Blender's segmentation capabilities to separate the AAA from the adjacent image. This procedure necessitates meticulous diligence to precisely delineate the aneurysm's limits. The 3D Reconstruction step employs segmented photos to generate a three-dimensional model of the AAA in Blender. This model offers a visual depiction of the aneurysm, allowing for examination and manipulation from multiple perspectives. The 3D printing procedure entails the fabrication of a tangible 3D model via an MSLA 3D printer. This entails utilizing Lychee software to create support for the model to guarantee effective printing. The CFD simulation phase entails loading the digital 3D models (normal aorta and aorta with aneurysm) into ANSYS software for computational fluid dynamics analysis. This will entail assessing blood characteristics, defining realistic boundary conditions, and simulating blood flow to evaluate flow patterns, pressure distribution, and wall shear stress.

Quality assurance standards are established during the process to ensure the accuracy and reliability of the 3D models. The metrics encompass the evaluation of segmentation error (SegE), digital editing error (DEE), and printing error (PrE). This methodology offers a thorough approach to generating patient-specific 3D printed models of AAAs, producing valuable insights into the characteristics and dynamics of AAAs, and facilitating the

formulation of tailored treatment strategies. The subsequent sections will provide a comprehensive review of each phase.

3.2 Research Design

The research approach utilized to develop patient-specific 3D printed models of Aortic Artery Aneurysms (AAA) using CT scan pictures adheres to an experimental design. The initial phase of the research design entails data gathering, particularly the acquisition of high-resolution spiral CT angiography images of the patient's aorta. This phase is crucial, as the accuracy of these pictures directly influences the fidelity of the final 3D model. The second part involves data processing, encompassing image segmentation and three-dimensional reconstruction utilizing Blender. Image segmentation entails extracting the AAA from the surrounding image via specialized tools in Blender.

The segmented data is subsequently utilized to generate a three-dimensional reconstruction of the AAA. The subsequent process entails the fabrication of the 3D model with 3D printing technology. The selection of printer and material may vary based on the model's attributes, including size, intricacy, and precision requirements. The concluding phase entails employing the 3D model for computational fluid dynamics simulation. The 3D models are generated from Blender and subsequently integrated into ANSYS to conduct simulations of blood flow within the abdominal aortic aneurysm (AAA). This approach is performed utilizing Computational Fluid Dynamics (CFD) and Finite Volume methods to solve the Navier-Stokes equations, which describe fluid motion in three-dimensional space.

During the research phase, quality assurance techniques are employed to guarantee the precision and dependability of the 3D models. The measures encompass evaluating segmentation error (SegE), digital editing error (DEE), and printing error (PrE). This methodological approach enables the fabrication of patient-specific 3D printed models of abdominal aortic aneurysms (AAAs), improving understanding of their characteristics and behaviors, and assisting in the formulation of individualized treatment plans.

3.3 Proposed Methodology

The methodology commences with image acquisition, securing high-resolution spiral CT angiography pictures of the patient's aorta. The quality of these photos is essential as it directly influences the precision of the final 3D model. It is imperative to take the

photographs in a manner that highlights the AAA and its adjacent structures. The CT scan images are subsequently imported into Blender, where segmentation methods are employed to delineate the AAA from the surrounding imagery. This approach necessitates careful diligence to precisely document the complex geometry of the AAA, encompassing its dimensions, configuration, and the size of the aneurysm. Numerous iterations and modifications may be required to precisely depict the AAA.

Following picture segmentation, the resultant segmented images are utilized to create a three-dimensional reconstruction of the abdominal aortic aneurysm (AAA) in Blender. The resultant 3D model must precisely represent the patient's AAA and can be viewed and manipulated from multiple angles to achieve a thorough comprehension of the aneurysm. The 3D model is subsequently exported from Blender in a compatible format for Lychee. It is imported into Lychee to create the requisite supports for effective printing. The 3D model is produced via an MSLA 3D printer and the selected printing medium.

The final phase entails CFD simulation. The 3D models (normal and aneurysmal aorta) are produced from Blender in a compatible format for ANSYS and subsequently integrated into the software. The 3D models are utilized to do simulations of blood flow in the aorta. This procedure is executed via Computational Fluid Dynamics (CFD) and Finite Volume methods to resolve the Navier-Stokes equations, which characterize fluid motion in three-dimensional space. Blood is classified as an incompressible and Newtonian fluid. A time-varying velocity waveform is imposed at the inlet border to replicate transient flow. This complex methodology can provide significant insights into the traits and behaviors of AAAs and can aid in developing tailored treatment strategies.

3.3.1 Experimental Setup for 3D Printed Models from CT scan images

3D printing is a complex process that necessitates careful consideration of numerous elements to provide accurate and secure results. The parameters can be categorised into nine sections: design, material, printer characteristics, post-processing, application-specific, quality control, software, regulatory, and environmental. The design parameters encompass anatomical accuracy, file format, scale, wall thickness, material compatibility, transparency/opaque-ness, sterilizability, biocompatibility, mechanical properties, and sterilizability.

The material parameters encompass biocompatibility, mechanical properties, transparency, and sterilizability. The printer's parameters encompass resolution, layer height, print speed, extruder temperature, and bed temperature. Cleaning, surface finishing, and assembly are examples of post-processing parameters, along with application-specific qualities such as surgical planning and educational models. The quality parameters encompass software parameters such as support structures, fill density and pattern, slicing software settings, as well as mechanical and biocompatibility evaluations.

Regulations are essential in the process, as they involve overseeing the printing environment, documenting design and manufacturing procedures for regulatory assessment, and complying with medical device standards. Controlled humidity and temperature are among the environmental elements, as are safety precautions such as correct ventilation and procedures for dealing with specific powders or resins.

The process of 3D printing a human aneurysm aortic artery from CT scanner pictures requires a range of specialised equipment and tools. These include medical imaging equipment, image processing and modelling equipment, 3D printing equipment, post-processing equipment, quality control and measurement equipment, safety equipment, documentation, and data management equipment, as well as miscellaneous equipment. Comprehending and following these criteria will allow for the accurate, efficient, and safe use of 3D-printed models in many applications.

3.3.1.1 Parameters

Undoubtedly, 3D printing is a multifaceted process that necessitates meticulous attention to a multitude of factors to guarantee secure and precise outcomes. The parameters can be divided into nine categories: design, material, printer characteristics, post-processing, application-specific, quality control, software, regulatory, and environmental (Marconi, Alaimo, & Mauri, 2022).

Anatomical accuracy, file format, scale, wall thickness, material compatibility, transparency/opaqueness, sterilizability, biocompatibility, and mechanical properties are all included in the design parameters (Bertolini, Rossoni, & Colombo, 2021). Material parameters encompass sterilizability, transparency, mechanical qualities, and biocompatibility (Bicudo, Faulkner, & Li, 2020).

Resolution, layer height, print speed, extruder temperature, and bed temperature comprise printer characteristics (Branzan et al., 2021). Activities such as surface finishing, cleaning, and assembly are included in post-processing parameters (Capelli, Bertolini, & Schievano, 2023). Surgical planning and educational models are also included in the application-specific aspects (Cardiac Computed Tomography Angiography (CCTA), 2023).

The equipment includes medical imaging equipment, image processing and modelling equipment, 3D printing equipment, post-processing equipment, quality control and measurement equipment, safety equipment, documentation and data management equipment, and miscellaneous equipment (Hagen et al., 2022). The precise, effective, and secure use of 3D-printed models in a variety of applications will be facilitated by the comprehension and adherence to these standards (Mørup, Stowe, Precht, Gervig, & Foley, 2022).

Table 3.1 summarizes essential parameters for 3D printing, including design, material, printer, post-processing, application-specific, quality control, software, regulatory, and environmental aspects

Category	Parameters
Design	Anatomical accuracy, File format, Scale, Wall thickness, Material compatibility, Transparency/Opaqueness, Sterilizability, Biocompatibility, Mechanical properties, Sterilizability
Material	Biocompatibility, Mechanical properties, Transparency, Sterilizability
3D Printer	Resolution, Layer height, Print speed, Extruder temperature, Bed temperature
Post-Processing	Cleaning, Surface finishing, Assembly
Application-Specific	Surgical planning, educational models

Quality Control	Software parameters (support structures, fill density, pattern, slicing software settings), Mechanical evaluations, Biocompatibility evaluations
Software	Support structures, fill density, Pattern, Slicing software settings
Regulatory	Printing environment oversight, Documentation for regulatory assessment, Compliance with medical device standards
Environmental	Controlled humidity, Controlled temperature, Safety precautions (ventilation, handling powders/resins)

3.3.1.2 Equipment

The procedure of 3D printing a human aneurysm aortic artery from CT scanner images is efficient and accurate, meeting the requirements for both research and clinical applications (Bertolini, Rossoni, & Colombo, 2021; Branzan et al., 2021). The equipment and tools utilised in this process can be categorised into medical imaging equipment, image processing and modelling equipment, 3D printing equipment, post-processing equipment, quality control and measurement equipment, safety equipment, documentation and data management equipment, and miscellaneous equipment. A CT scanner is used to obtain precise images of the aorta artery (Cardiac Computed Tomography Angiography, 2023; Hagen et al., 2022). The image processing and modelling equipment comprises a computer workstation dedicated to processing CT images and generating 3D models (Mørup et al., 2022; Song et al., 2022). Software such as Blender, MeshLab, or Autodesk Meshmixer is used to enhance and perfect 3D models (PRECISE3DM, 2021).

3D printing equipment includes a range of devices, such as a 3D printer, an FDM (Fused Deposition Modelling) printer, an SLA (Stereolithography) printer, and PolyJet Printer, which are used for creating multi-material and intricately detailed models (Chen et al., 2023; Marconi et al., 2022). Printing materials consist of biocompatible resins or filaments that are used to create precise and safe models (Muskan, Gupta, & Negi, 2022).

Additionally, support materials are used to print intricate structures (Teaching Tech, 2020). The post-processing equipment comprises an ultrasonic cleaner, a curing station, and polishing instruments for surface finishing (Chen et al., 2023). Quality control and measurement tools such as calculators and micrometres are used to measure the dimensions of the printed models, as well as a 3D scanner to ensure that the printed models are accurate when compared to the original 3D models (Mørup et al., 2022). Safety equipment encompasses protective attire, ventilation systems, and documentation software for comprehensive process monitoring (Daly, 2023).

Table 3.2 summarises the equipment and tools necessary for efficiently and accurately 3D printing a human aneurysm aortic artery from CT scanner images, meeting both research and clinical application requirements.

Category	Equipment/Tools
Medical Imaging Equipment	CT scanner
Image Processing and Modelling Equipment	Computer workstation, Software (Blender, MeshLab, Autodesk Meshmixer)
3D Printing Equipment	3D printer, FDM (Fused Deposition Modelling) printer, SLA (Stereolithography) printer, PolyJet printer, Biocompatible resins/filaments, Support materials
Post-Processing Equipment	Ultrasonic cleaner, Curing station, Polishing instruments
Quality Control and Measurement Equipment	Calculators, Micrometres, 3D scanner
Safety Equipment	Protective attire, Ventilation systems, Documentation software
Documentation and Data Management Equipment	Documentation software

Miscellaneous Equipment	Additional tools as required
----------------------------	------------------------------

3.4 Limitation of Proposed Methodology

The suggested approach for generating patient-specific 3D printed replicas of Aortic Artery Aneurysms (AAA) from CT scan images, although showing potential, does possess certain constraints.

A significant limitation is the difficulty in guaranteeing quality assurance. The overall error in patient-specific anatomical models is composed of three significant partial errors in the production process: segmentation error (SegE), digital editing error (DEE), and printing error (PrE). The insufficient discriminatory capacity of certain assessment methods poses a challenge when comparing results. The current approaches to ensure the quality of segmentation are typically categorised as either realistic and accurate or resource-efficient (Schulze et al., 2024).

Another constraint is the requirement for standardisation. With the growing prevalence of 3D printed models in medical education, there is an increasing need for standardised evaluation. A comprehensive literature review has identified a total of one hundred questions that were previously published in surveys that evaluated patient-specific 3D models for the purpose of surgical planning. A conclusive survey comprising twenty inquiries was formulated (Schlegel et al., 2022).

Moreover, the analysis of CT scans can present difficulties. FEVAR cases pose challenges due to the complexity of interpreting CT scans and CT three-dimensional reconstruction, which may not accurately depict the anatomical structure of the aorta. These challenges can result in either an overestimation or underestimation of the examined errors (Schulze et al., 2024).

Furthermore, the selection of 3D printing technology and materials may impose certain restrictions. Both the lost mould and lost core techniques are researched and employed in the production of the AAA models. The article provides a comprehensive description of the design and fabrication phases, including details on costs and equipment

requirements. It also discusses the primary benefits and limitations of the proposed methodologies (Frontiers, 2023).

3.5 Summary

This study employs CT images to generate patient-specific three-dimensional printed models of Aortic Artery Aneurysms (AAAs). The procedure entails obtaining high-resolution spiral CT angiography pictures and employing specialized software to process these images, thereby producing a 3D model. Computational Fluid Dynamics (CFD) and Finite Volume methods are utilized to model blood flow within the abdominal aortic aneurysm (AAA). This CFD research elucidates blood flow patterns and pressures within the aneurysm, offering significant insights into its dynamics. A compatible printer and material are chosen according to model specifications, and the 3D model is fabricated.

Generating precise 3D printed models from CT scans necessitates meticulous attention to multiple parameters. These encompass design factors including anatomical accuracy, file format, scale, and wall thickness. The selection of materials is essential, considering characteristics such as compatibility, transparency, sterilizability, biocompatibility, and mechanical capabilities. The characteristics of the selected printer, such as resolution, layer height, print speed, and temperature settings, are also crucial factors. Post-processing processes, including cleaning, surface finishing, and assembly, are crucial for enhancing the final product. Moreover, stringent quality control protocols are essential to guarantee the precision and dependability of the models. The measures entail evaluating support structures, fill density, pattern, slicing software configurations, and performing mechanical and biocompatibility assessments.

CHAPTER 4

RESULTS AND DISCUSSIONS

4.1 Introduction

This study investigates the utilization of 3D printing technology to produce precise, patient-specific models of aortic artery aneurysms (AAA). The procedure commences with the acquisition of high-resolution CT scan images, which are ethically obtained and anonymized to safeguard patient confidentiality. The images are segmented to isolate the aorta from adjacent anatomical structures using software tools (Bertolini et al., 2021). This segmented data is utilized to create a digital 3D model of the aorta, precisely representing the patient's distinct anatomy and the particular attributes of the aneurysm.

The 3D model is subsequently refined with 3D modelling software, such as Blender, to improve its quality by smoothing surface irregularities, filling minor gaps or holes, and rectifying inaccuracies to ensure an accurate representation of the aneurysm's intricate morphology. The polished digital model is subsequently imported into specialized slicing software to ready it for 3D printing. The 3D printing process employs Stereolithography (SLA) technology using a high-resolution 3D printer, like the Anycubic Photon M3 Max, recognized for its capacity to create complex and detailed models. The printing material is a robust resin specifically designed for SLA printing, selected for its characteristics that closely replicate the mechanical properties of an actual blood vessel.

Additionally, the digital model can facilitate computational fluid dynamics (CFD) simulations to examine blood flow patterns, pressure distribution, and wall shear stress within the aneurysm (Etli et al., 2020; Simão et al., 2017). This information is essential for comprehending aneurysm behavior and devising treatment strategies. Quality control measures are instituted throughout the entire process, from image acquisition to CFD analysis, to guarantee the accuracy, reliability, and validity of the outcomes. This entails meticulous verification of initial medical images, guaranteeing their quality and resolution are adequate for precise segmentation and 3D reconstruction. The assessment of 3D printed models and CFD simulation outcomes can augment medical education by offering concrete

and interactive resources for students and professionals to examine and comprehend the intricacies of aortic aneurysms.

4.2 3D-Printed Model of Patient-Specific Aortic Artery Aneurysms

The journey from a series of 2D CT scan images to a 3D printable CAD model is a meticulous one. It commenced with the careful selection of appropriate CT scan images, ensuring they captured the intricate details of the aorta and the aneurysm. These images were then imported into specialized 3D modelling software, where the process of segmentation took place. Much like a sculptor chiselling away excess stone to reveal the form within, I meticulously isolated the aorta from the surrounding anatomical structures in each image. This process required patience and precision, ensuring that the boundaries of the aorta were accurately defined. The segmented images were then woven together, like threads in a tapestry, to construct the 3D model. This digital representation of the aorta, now ready for printing, accurately reflected the patient's unique anatomy.

Aortic artery aneurysms (AAAs) are a critical condition characterized by the weakening and outward bulging of the aortic wall. Early detection and treatment planning are crucial to prevent life-threatening complications. The integration of medical imaging and 3D printing technologies has shown exciting potential for improving diagnostic accuracy, surgical planning, and patient outcomes. This essay describes the process of creating 3D-printed models of patient-specific aortic artery aneurysms using CT scan images.

4.2.1 Process

The 3D printing process involves acquiring medical images of a human aorta, segmenting them, reconstructing a 3D model, and refining the model using Blender. The model is then printed using a high-resolution printer like Anycubic Photon M3 Max, and post-processed for quality control. The results are then used for Computational Fluid Dynamics (CFD) simulation to understand blood flow dynamics within the aneurysm. The process contributes to medical education, surgical planning, and research in vascular health.

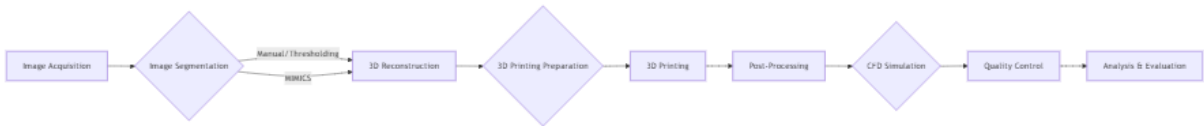


Figure 4.1 shows the flowchart of the whole process

4.2.2 Image Acquisition

The process commences with the acquisition of high-resolution medical images, typically in the form of Computed Tomography (CT) scans, highlighting a human aorta with an aneurysm. These images serve as the foundational dataset for the entire project, providing a detailed visualization of the patient's anatomy and the specific characteristics of the aneurysm. Ethical considerations and patient privacy are paramount; therefore, the images are sourced responsibly, either from anonymized patient datasets, publicly available research databases, or collaborations with medical professionals who ensure proper de-identification procedures are followed. The quality and resolution of these images are critical, as they directly impact the accuracy and detail of the subsequent 3D model.

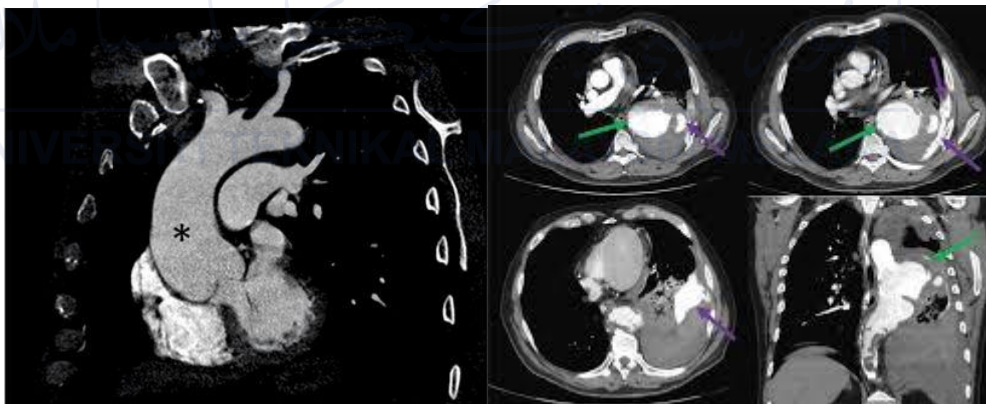


Figure 4.2 shows the CT Scan of images of Human Normal Aorta (Left) and Aneurysm Aorta (Right)

4.2.3 Image Segmentation

Once the CT scan images are obtained, they undergo a crucial step known as segmentation. This process involves utilizing specialized software tools to meticulously isolate the region of interest – the aortic aneurysm – from the surrounding anatomical structures. This isolation

is achieved through a combination of automated techniques, such as thresholding, which separates objects based on pixel intensity, and region growing, which expands a selected region based on shared characteristics. However, manual editing is often necessary to refine the segmentation and ensure precise delineation of the aneurysm's boundaries. This meticulous segmentation process results in a 3D digital representation of the aneurysm, accurately capturing its shape, size, and location within the aorta.

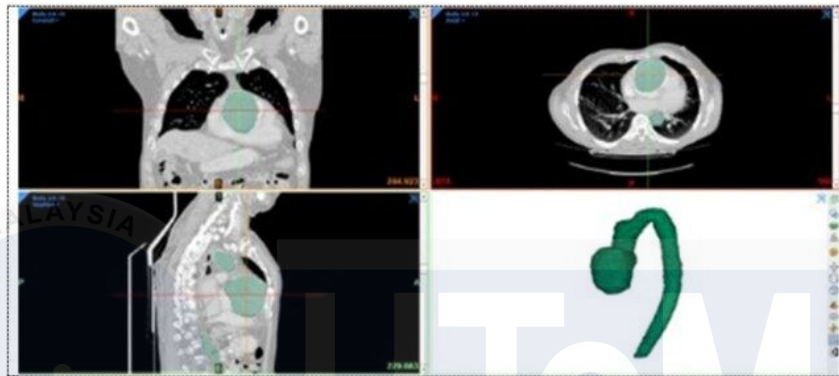


Figure 4.3 shows the interface of MIMICS software and how the image segmented.

4.2.4 3D Reconstruction

With the segmented aneurysm data ready, the next stage involves reconstructing a comprehensive 3D model of the affected aorta. This reconstruction process utilizes advanced medical imaging software, such as Materialise Mimics, which is specifically designed to convert segmented image data into accurate 3D representations. The software algorithms analyze the segmented slices and generate a continuous 3D surface model of the aneurysm, providing a tangible visualization of its complex geometry. This 3D model serves as the digital blueprint for the subsequent 3D printing process, enabling the creation of a physical replica for further analysis and investigation.

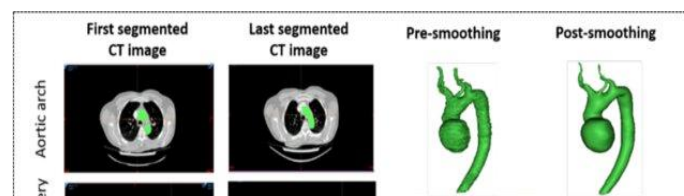


Figure 4.4 illustrates how the 3D model was reconstructed.

4.2.5 3D Model Refinement using Blender Software

The 3D model generated from the medical imaging software, while anatomically accurate,

may contain minor imperfections or artifacts resulting from the segmentation or reconstruction process. To address this, the model is imported into Blender, a powerful open-source 3D creation suite. Blender’s versatile sculpting tools are employed to further refine the model, ensuring its suitability for 3D printing. This refinement process involves smoothing out any remaining surface irregularities, filling in small gaps or holes, and correcting any inaccuracies that might affect the printed output. By utilizing tools like the “Smooth” brush, “Grab” tool, and “Snake Hook” brush, the model is meticulously refined to achieve a high level of detail and precision, ensuring a faithful representation of the aneurysm’s complex morphology.

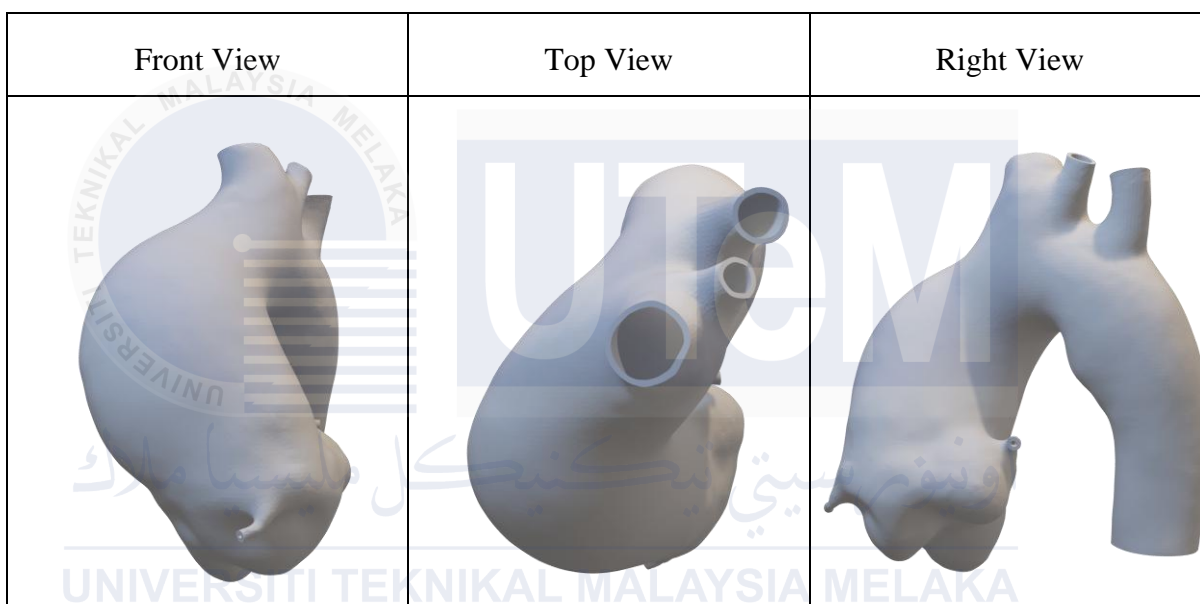


Table 4.1 Shows the front view, top view, and right view of the Aneurysm Aorta

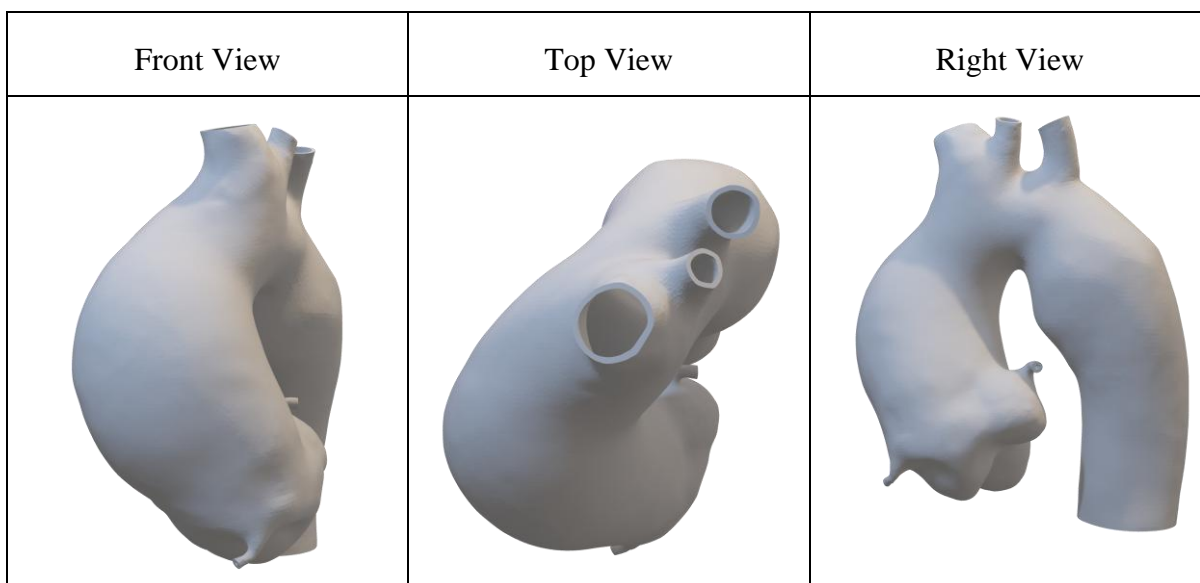


Table 4.2 Shows the front view, top view and right view of the Normal Aorta

4.2.6 Supports making for 3D Printing using Lychee Software

Before the refined 3D model can be physically realized through 3D printing, it undergoes a crucial preparation stage. This stage involves importing the model into specialized slicing software, such as Lychee Slicer, which is specifically designed for preparing models for resin-based 3D printing. Within Lychee, the model is carefully analyzed, and support structures are strategically generated and added. These supports are essential for ensuring that intricate features, overhangs, and complex geometries are printed accurately without collapsing or warping during the printing process. The parameters of these supports, such as their density, contact point size, and overall strength, are meticulously adjusted to provide optimal stability while also ensuring easy removal after printing. This meticulous preparation ensures that the 3D printing process yields a high-quality, accurate representation of the aneurysm.

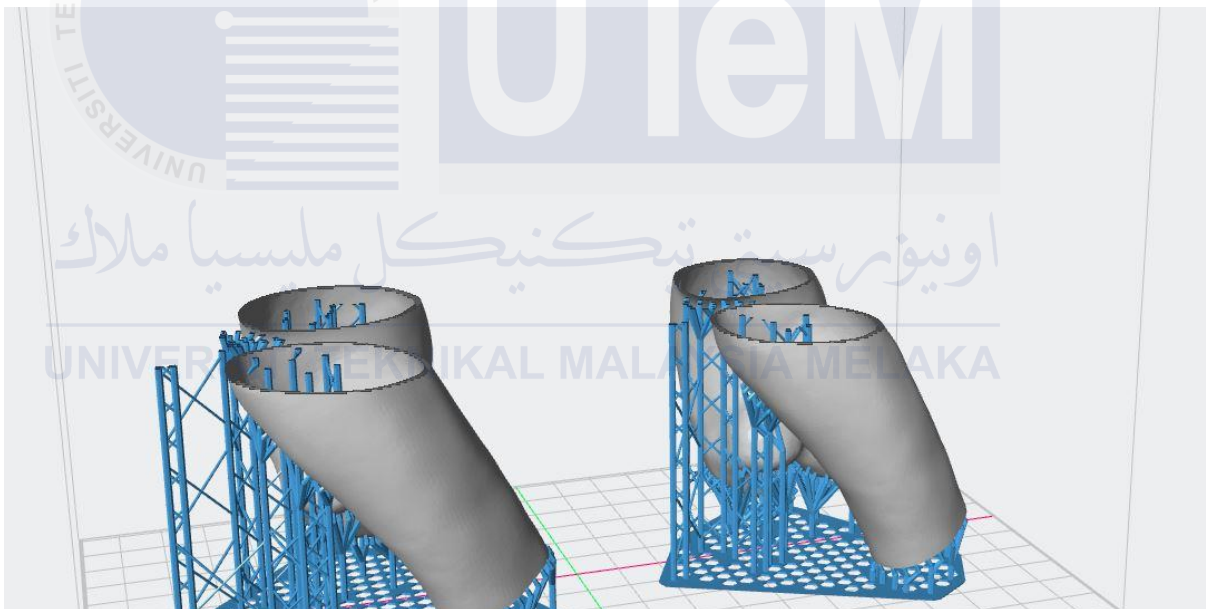


Figure 4.5 shows the support making process for 3D Printing.

4.2.7 3D Printing Process

With the 3D model fully prepared, the actual printing process commences. The chosen 3D printer for this project is the Anycubic Photon M3 Max, a large-format MSLA (Masked Stereolithography) printer renowned for its high resolution and ability to produce intricate and detailed models. The printer's large build volume is particularly important for accommodating the full size of the aneurysm models. The printing material selected is Anycubic Tough Resin Ultra, a resin specifically formulated for MSLA printing and chosen

for its unique properties that closely mimic the mechanical behavior of a real blood vessel. Its high tensile strength ensures durability and the ability to withstand handling, while its impressive elongation at break provides the necessary flexibility to simulate the natural movement of an artery. Additionally, the resin's impact resistance safeguards the model from potential damage during handling or future simulations. The printing process itself involves several key steps: platform leveling to ensure the correct distance between the build platform and the resin vat, filling the vat with the chosen resin, transferring the prepared model file to the printer, and initiating the automated printing process, where the resin is cured layer by layer according to the digital model. This combination of advanced 3D printing technology and carefully selected materials aims to produce accurate, detailed, and functionally representative 3D printed models of aortic aneurysms.

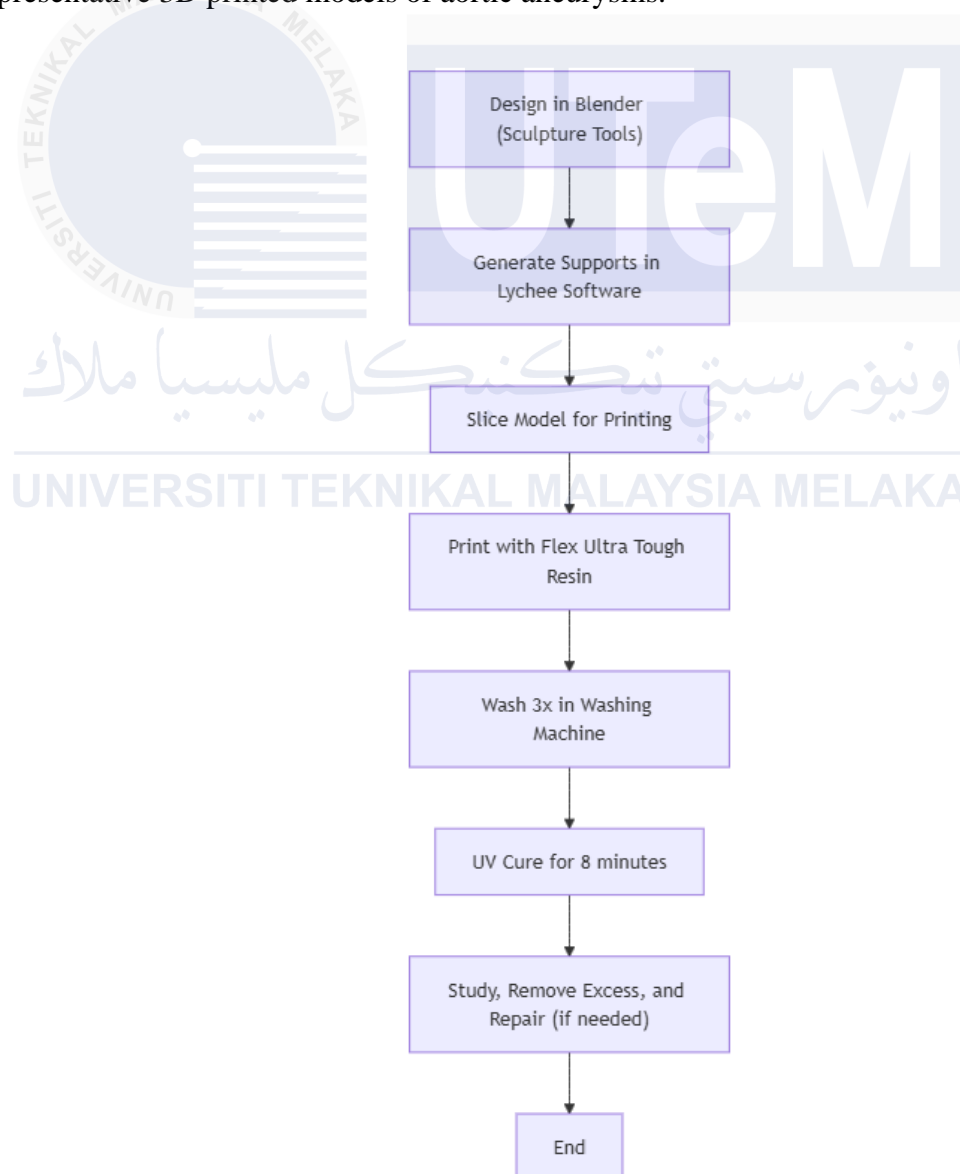


Figure 4.6 shows a flowchart of the 3D Printing Process

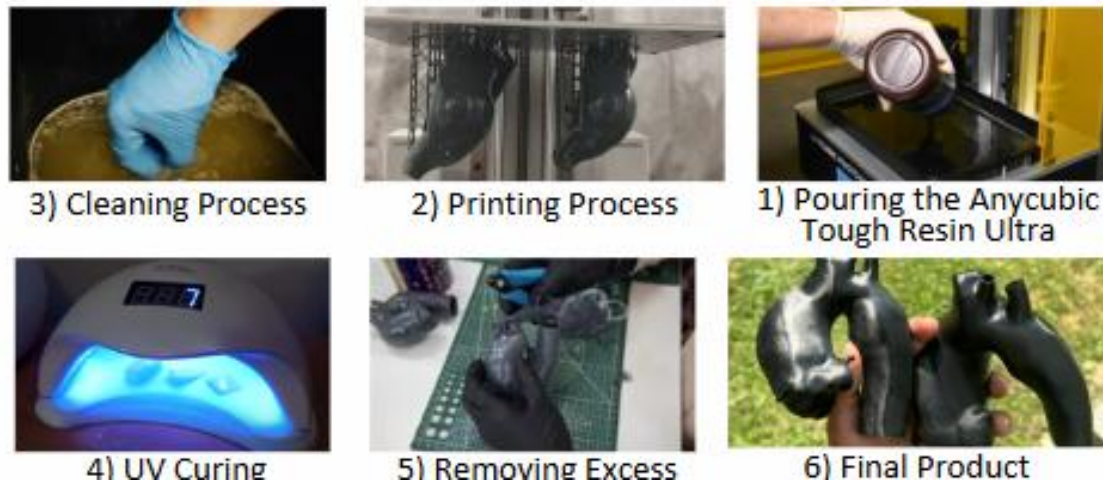


Figure 4.7 shows the documentation for each part of the 3D Printing Process

4.2.8 Post-Processing

Once the 3D printing process is complete, the printed aneurysm models undergo a series of post-processing steps to finalize their form and ensure their quality. This involves carefully removing the support structures that were essential during printing but are no longer needed. The models are then thoroughly cleaned to remove any residual resin, ensuring a smooth and pristine surface finish. Depending on the desired level of realism and the intended application of the models, additional post-processing techniques may be employed.



Figure 4.8 shows the Post-Processing Activities

4.3 3D Printed Model

3D printing of human aneurysm aortic artery using CT scan images involves creating a three-dimensional model of an aortic aneurysm using CT scan data. This process allows for visualization of the aneurysm and surrounding structures, aiding in medical education.



Figure 4.9 shows The final replicas from 3D Printing.

4.4 CAD Model Preparation and Comparison by CFD Analysis

The application of Computer-Aided Design (CAD) software has transformed the product development process in engineering and design. CAD models offer a digital depiction of tangible items, allowing engineers to visualize, analyze, and enhance designs prior to production. This essay explores the complexities of CAD model preparation, highlighting the importance of Computational Fluid Dynamics (CFD) analysis in assessing and contrasting design iterations, specifically regarding aortic blood flow analysis, referencing a recent study published in MDPI.

The development of CAD models is an essential phase in the CFD analysis process. Thorough preparation guarantees the precision and dependability of simulation outcomes, allowing engineers to make educated design choices. CFD analysis enables me to assess performance, enhance designs, and undertake comparative analyses, resulting in superior product functionality, efficiency, and creativity. As CFD tools and methodologies progress, their incorporation with CAD software will enhance the design process, promoting the creation of high-performance products across several industries. The utilization of CFD to comprehend aortic blood flow dynamics, as illustrated in this essay and corroborated by subsequent studies, shows the efficacy of this technology in tackling significant difficulties in healthcare and engineering.

4.4.1 CAD Model Preparation

The development of a CAD model frequently constitutes the preliminary phase in the design process. I utilized CAD software to create 2D sketches and 3D models, specifying the geometry and dimensions of the proposed product. Prior to subjecting a CAD model to CFD analysis, it necessitates thorough preparation to guarantee precise and dependable simulation outcomes.

Complex CAD models frequently incorporate delicate features, like minor gaps, fillets, and chamfers, which can elevate computational expenses and even induce numerical instability in CFD simulations. To resolve this, I streamlined the geometry by eliminating or idealizing certain features, while maintaining the fundamental flow properties of the model.

CFD analysis requires the establishment of a computational domain, which delineates the physical space surrounding the CAD model where fluid dynamics are simulated. The scope must be adequately expansive to encompass the pertinent flow events without imposing an undue computational load.

Mesh generation entails discretizing the computing domain into smaller pieces, such as tetrahedra or hexahedra. The caliber of the mesh profoundly affects the precision and stability of the CFD simulation. I meticulously regulated mesh density and distribution to guarantee sufficient resolution of flow characteristics, especially in areas with steep gradients.

4.4.2 Computational Fluid Dynamics (CFD) Analysis

CFD analysis is essential for assessing and contrasting several iterations of CAD models. Engineers can acquire insights into essential performance metrics, like pressure drop, flow distribution, and heat transfer, by simulating fluid flow around or through the models. This information allows me to detect design deficiencies, enhance performance, and choose the most appropriate design among multiple options.

CFD simulations yield quantitative insights into the fluid dynamic characteristics of the CAD model. This data can evaluate the model's performance relative to design specifications and pinpoint areas for enhancement. In the design of a piping system, CFD analysis can identify zones of significant pressure loss or flow recirculation, highlighting potential issues.

CFD analysis functions as a potent instrument for design optimisation. Through iterative modifications of the CAD model and performance evaluation via CFD simulations, I may systematically enhance the design to meet specified performance objectives. This iterative method can result in substantial enhancements in efficiency, reliability, and overall design quality.

CFD analysis allows engineers to perform comparison studies when faced with several design possibilities. By replicating the performance of each design under uniform settings, I can objectively evaluate their advantages and disadvantages. This comparison can assist in identifying the best appropriate design based on measurable performance criteria.

4.4.3 ANSYS Fluent Setup for Aortic Blood Flow Simulation

Drawing upon a recent study published in MDPI, which highlights the importance of CFD in understanding the hemodynamic of aortic aneurysms, particularly the relationship between wall shear stress (WSS) and aneurysm growth, this section details the ANSYS Fluent setup used to simulate blood flow in an aorta model.

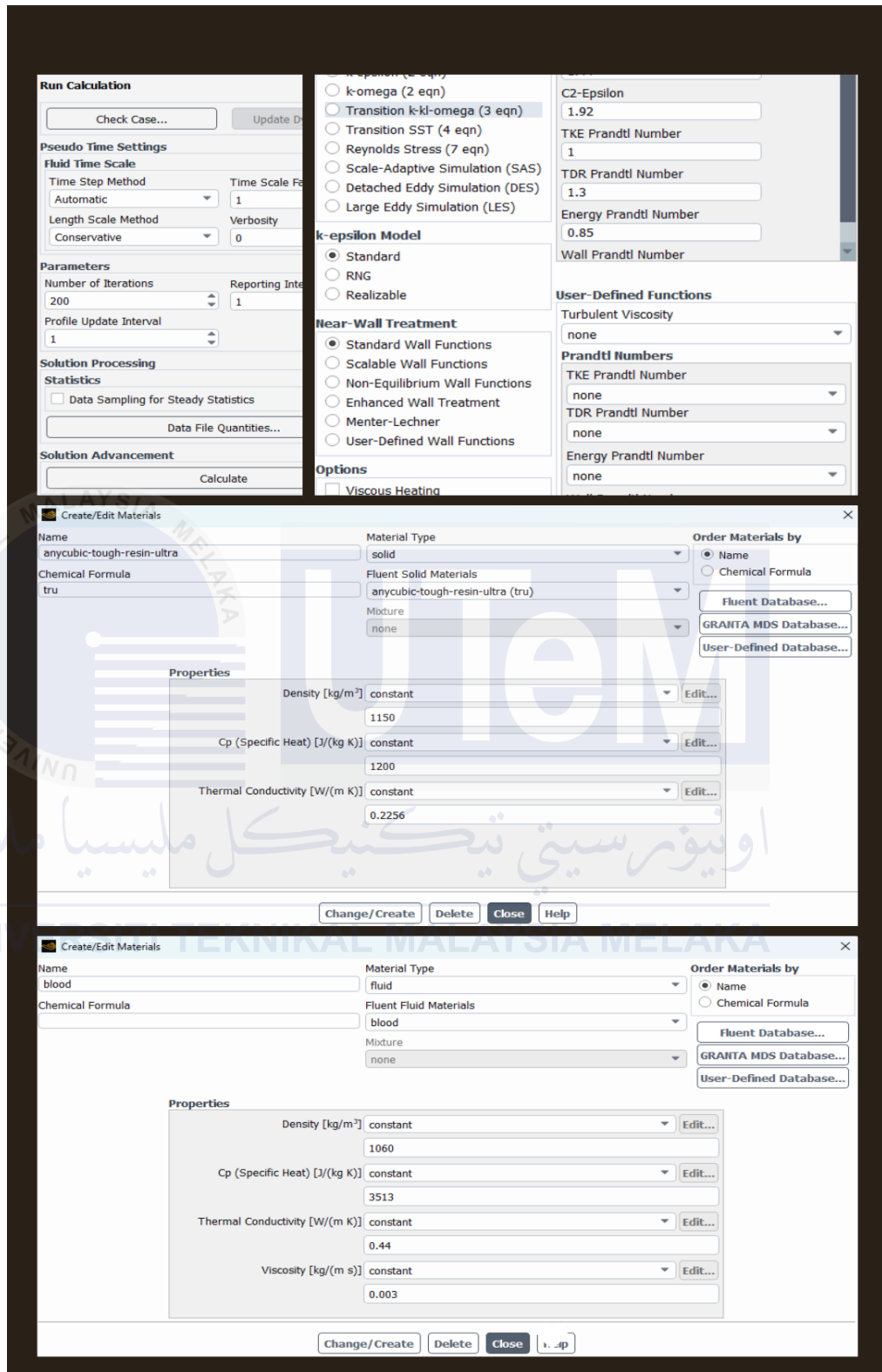


Figure 4.10 A summary of setup in the ANSYS Fluent

A pressure-based solution appropriate for incompressible flows, such as blood, was utilised, as indicated in Figure 4.5. The k- ω SST turbulence model was selected for its

capacity to accurately represent intricate flow patterns, such as flow separation and reattachment, pertinent to aortic blood flow. The fluid was characterised as 'blood' with corresponding density and viscosity characteristics, while 'anycubic-tough-resin-ultra' presumably denotes the material designated for the aorta model.

The model shape seems to feature one inlet and several outlets ('outlet_1' to 'outlet_4'), indicating a depiction of vascular branching. The 'wall' boundary presumably delineates the aortic wall. The simulation was executed for 200 iterations. The fluid zone, designated as 'part1_blum_cfd_', employs 'blood' as its substance. The energy equation is activated, signifying the incorporation of heat transfer in the simulation.

Subsequent investigations will concentrate on contrasting essential haemodynamic measures, including wall shear stress (WSS), velocity profiles, and pressure distribution, with the findings presented in the MDPI study. This comparison research will confirm the simulation design and elucidate the potential clinical implications of the findings.

4.4.4 CFD Simulation Results

CFD simulations are a crucial tool in CFD analysis, providing engineers with insights into pressure drop, flow distribution, and heat transfer in CAD models. These simulations help identify design deficiencies, enhance performance, and select the most suitable design. CFD analysis also aids in design optimization by systematically enhancing the model to meet performance objectives. By replicating the performance of various design possibilities, engineers can identify the best appropriate design based on measurable performance criteria.

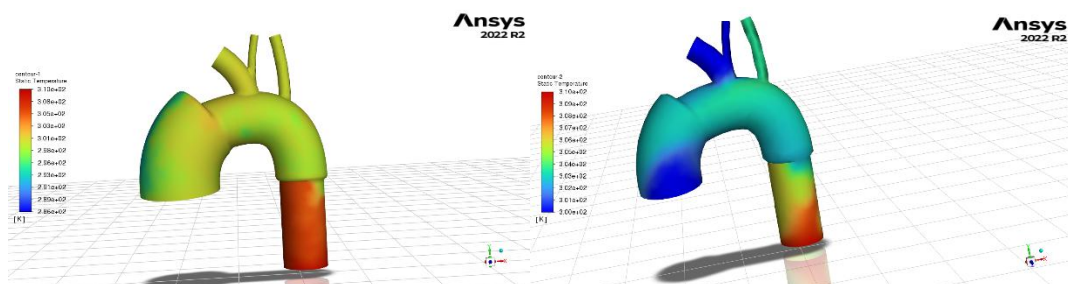


Figure 4.11 shows the Wall Shear Stress Contours for Aneurysm Aorta (Left) and Normal aorta (Right)

CHAPTER 5

CONCLUSION

This study aimed to improve the educational experience for students, researchers, and academics in the medical domain by employing 3D printing technology and computational fluid dynamics (CFD) to visualize and analyze aorta artery aneurysms (AAA). The research had three main objectives. The first was to convert CT scan data into a 3D printable STL file format. This entailed utilizing software to analyze CT scan pictures and generate a 3D model suitable for printing. The resultant STL file would be utilized to build instructional 3D printed models of the aorta.

The second objective was to three-dimensionally print at least two models for comparative analysis: one depicting a normal aorta and the other illustrating an aorta with an aneurysm. This would facilitate a visible and physical comparison of the two circumstances, enhancing the comprehension of the anatomical variations induced by the aneurysm.

The third objective was to employ computational fluid dynamics (CFD) studies to illustrate the impact of an aneurysm on haemodynamics. This would entail modeling blood flow in both normal and aneurysmal aorta models to visualize and analyze the wall shear stress. The CFD results would elucidate the haemodynamics changes linked to AAA, hence enriching the educational experience for students, researchers, and scholars.

The study successfully achieved the objectives. CT scan data was converted into a 3D printable STL file format, and two models were printed: one depicting a normal aorta and the other illustrating an aorta with an aneurysm.

In future research, efforts should focus on simplifying the CAD model to enable the use of CFD analysis for studying the impact of an aneurysm on hemodynamics. This information can be used to further understand the behavior of the aneurysm and to plan treatment strategies. Additionally, exploring the use of 3D-printed models for other educational purposes, such as teaching patients about their own anatomy or training surgeons on new surgical techniques, could be beneficial.

REFERENCES

- Abdominal & Thoracic Aortic Aneurysm Treatment: Open Surgery | Q&A. (n.d.). [Video]. Retrieved from <https://clinicalconnection.hopkinsmedicine.org/videos/abdominal-and-thoracic-aortic-aneurysm-treatment-open-surgery-qanda>
- Bertolini, M., Rossoni, M., & Colombo, G. (2021). Operative Workflow from CT to 3D Printing of the Heart: Opportunities and Challenges. *Bioengineering*, 8(10), 130. <https://doi.org/10.3390/bioengineering8100130>
- Bicudo, E., Faulkner, A., & Li, P. (2020). Patents and the experimental space: social, legal and geographical dimensions of 3D bioprinting. *International Review of Law Computers & Technology*, 35(1), 2–23. <https://doi.org/10.1080/13600869.2020.1785066>
- Branzan, D., Geisler, A., Grunert, R., Steiner, S., Bausback, Y., Gockel, I., Scheinert, D., & Schmidt, A. (2021). The Influence of 3D Printed Aortic Models on the Evolution of Physician Modified Stent Grafts for the Urgent Treatment of Thoraco-abdominal and Pararenal Aortic Pathologies. *European Journal of Vascular and Endovascular Surgery*, 61(3), 407–412. <https://doi.org/10.1016/j.ejvs.2020.10.023>
- Capelli, C., Bertolini, M., & Schievano, S. (2023). 3D-printed and computational models: a combined approach for patient-specific studies. In Elsevier eBooks (pp. 105–125). <https://doi.org/10.1016/b978-0-323-89831-7.00011-0>
- Cardiac Computed Tomography Angiography (CCTA). (2023, May 3). Retrieved from <https://www.heart.org/en/health-topics/heart-attack/diagnosing-a-heart-attack/cardiac-computed-tomography>
- Chen, W., Fernandez, C. S., Xu, L., Velliou, E., Homer-Vanniasinkam, S., & Tiwari, M. K. (2023). High-resolution 3D printing for healthcare. In Elsevier eBooks (pp. 225–271). <https://doi.org/10.1016/b978-0-323-89831-7.00013-4>
- Daly, A. (2023). Medical 3D printing, intellectual property, and regulation. In Elsevier eBooks (pp. 385–398). <https://doi.org/10.1016/b978-0-323-89831-7.00014-6>
- Dr. Paulien Moyaert. (2023, March 1). What is an Aortic Aneurysm? | 3D Animation [Video]. YouTube. Retrieved from <https://www.youtube.com/watch?v=LSJQ6ckQc1M>
- Geng, J., Wang, Y., Ji, Z., Wang, W., Yin, Y., Yang, G., Fan, X., Li, T., Hu, P., He, C., & Zhang, H. (2023). Advantages of 3D registration technology (3DRT) in clinical application of unruptured intracranial aneurysm follow-up: A novel method to judge aneurysm growth. *Journal of Neuroradiology*, 50(2), 209–216.

<https://doi.org/10.1016/j.neurad.2022.08.004>

Göçer, H., Durukan, A. B., Tunç, O., Naser, E., Gürbüz, H. A., & Ertuğrul, E. (2021). Evaluation of 3D printing in planning, practicing, and training for endovascular lower extremity arterial interventions. *Türk Göğüs Kalp Damar Cerrahisi Dergisi :Türk Göğüs Kalp Damar Cerrahisi Dergisi*, 29(1), 20–26.

<https://doi.org/10.5606/tgkdc.dergisi.2021.20478>

Hagen, F., Hofmann, J., Wrazidlo, R., Gutjahr, R., Schmidt, B., Faby, S., Nikolaou, K., & Horger, M. (2022). Image quality and dose exposure of contrast-enhanced abdominal CT on a 1st generation clinical dual-source photon-counting detector CT in obese patients vs. a 2nd generation dual-source dual energy integrating detector CT. *European Journal of Radiology*, 151, 110325. <https://doi.org/10.1016/j.ejrad.2022.110325>

how does 3d printing work - Google Search. (n.d.). Retrieved from https://www.google.com/search?sca_esv=9b23b06c2ff3b9a3&sca_upv=1&sxsrf=ADL_YWILnNmYg-0IkEZEAEELk5zyYRwrsA:1717827400055&q=how+does+3d+printing+work&tbm=vid&source=lnms&prmd=ivsnbmtz&sa=X&ved=2ahUKEwiGwtzfrcuGAXVyyzgGHe8IPAUQ0pQJegQIFxAB&biw=718&bih=772&dpr=1#

Ludvigsen, K., Nagaraja, S., & Daly, A. (2021). When Is Software a Medical Device? Understanding and Determining the “Intention” and Requirements for Software as a Medical Device in European Union Law. *European Journal of Risk Regulation*, 13(1), 78–93. <https://doi.org/10.1017/err.2021.45>

Mahajan, N. N., Cicek, S. M., McGregor, C. G., Boland, J. M., Morris, J. M., Okuno, S. H., Robinson, S. I., White, D. B., Yi, E. S., & Blackmon, S. H. (2020). A Case Series of Long-Term Surgical Outcomes of Primary Pulmonary Artery Sarcomas With Opportunities for 3D-Printed Models in Surgical Planning. *Innovations*, 16(1), 94–100. <https://doi.org/10.1177/1556984520960716>

Marconi, S., Alaimo, G., Mauri, V., Negrello, E., & Auricchio, F. (2022). 3D printing technologies and materials in the medical field. In Elsevier eBooks (pp. 1–17). <https://doi.org/10.1016/b978-0-323-85430-6.00004-2>

Mørup, S. D., Stowe, J., Kusk, M. W., Precht, H., & Foley, S. (2022). The impact of ASiR-V on abdominal CT radiation dose and image quality – A phantom study. *Journal of Medical Imaging and Radiation Sciences*, 53(3), 453–459. <https://doi.org/10.1016/j.jmir.2022.06.008>

- Mørup, S., Stowe, J., Precht, H., Gervig, M., & Foley, S. (2022). Design of a 3D printed coronary artery model for CT optimization. *Radiography*, 28(2), 426–432. <https://doi.org/10.1016/j.radi.2021.09.001>
- Mubarik, A., Sharma, S., & Law, M. A. (2023, January 21). Bicuspid Aortic Valve. StatPearls - NCBI Bookshelf. Retrieved from <https://www.ncbi.nlm.nih.gov/books/NBK534214/#:~:text=A%20bicuspid%20aortic%20valve%20is,with%20dilatation%20of%20the%20aorta.>
- Muskan, N., Gupta, D., & Negi, N. P. (2022). 3D bioprinting: Printing the future and recent advances. *Bioprinting*, 27, e00211. <https://doi.org/10.1016/j.bprint.2022.e00211>
- PRECISE3DM. (2021, March 10). 3D Scan to CAD Modeling using Geomagic Design X - Reverse Engineering [Video]. YouTube. Retrieved from <https://www.youtube.com/watch?v=4Y5IICMBR8>
- Ross Procedure - Aortic Surgery. (n.d.). Mount Sinai Health System. Retrieved from <https://www.mountsinai.org/care/heart/services/aortic/surgery/ross>
- Santoro, G., Pizzuto, A., Rizza, A., Cuman, M., Federici, D., Cantinotti, M., Pak, V., Clemente, A., & Celi, S. (2021). Transcatheter Treatment of “Complex” Aortic Coarctation Guided by Printed 3D Model. *JACC. Case Reports*, 3(6), 900–904. <https://doi.org/10.1016/j.jaccas.2021.04.036>
- Schroeder, G., Edalati, M., Tom, G., Kuntjoro, N., Gutin, M., Gurian, M., Cuniberto, E., Hirth, E., Martiri, A., Sposato, M. T., Aminzadeh, S., Eichenbaum, J., Alizadeh, P., Baidya, A., Haghniaz, R., Nasiri, R., Kaneko, N., Mansouri, A., Khademhosseini, A., & Sheikhi, A. (2022). Assessing the aneurysm occlusion efficacy of a shear-thinning biomaterial in a 3D-printed model. *Journal of the Mechanical Behavior of Biomedical Materials/Journal of Mechanical Behavior of Biomedical Materials*, 130, 105156. <https://doi.org/10.1016/j.jmbbm.2022.105156>
- Song, Y., Du, X., Zhang, Y., & Li, S. (2022). Two-stage segmentation network with feature aggregation and multi-level attention mechanism for multi-modality heart images. *Computerized Medical Imaging and Graphics*, 97, 102054. <https://doi.org/10.1016/j.compmedimag.2022.102054>
- Söreljus, K., Wyss, T. R., Adam, D., Beck, A. W., Berard, X., Budtz-Lilly, J., Chakfé, N., Clough, R., Czerny, M., D’Oria, M., Dang, M., Di Summa, P. G., Eldrup, N., Fourneau, I., Heinola, I., Hosaka, A., Hsu, R. B., Huang, Y. K., Jutidamrongphan, W., . . . Weiss, S. (2023). Editor’s Choice – Infective Native Aortic Aneurysms: A Delphi Consensus

- Document on Terminology, Definition, Classification, Diagnosis, and Reporting Standards. *European Journal of Vascular and Endovascular Surgery*, 65(3), 323–329. <https://doi.org/10.1016/j.ejvs.2022.11.024>
- Teaching Tech. (2020, September 8). Essential (and obscure) 3D printing tools and spares [Video]. YouTube. Retrieved from <https://www.youtube.com/watch?v=XBoXp31PCo8>
- The Keyhole Heart Clinic. (2023, March 1). Bicuspid Aortic Valve: How Serious Is It Really? [Video]. YouTube. Retrieved from <https://www.youtube.com/watch?v=XZg8Su8ICeY>
- Types and Causes of Aortic Aneurysms. (n.d.). Mount Sinai Health System. Retrieved from <https://www.mountsinai.org/care/heart/services/aortic/types-causes>
- Uvahealth. (2021, June 4). Open Aortic Aneurysm Repair [Video]. YouTube. Retrieved from <https://www.youtube.com/watch?v=LIVkfMFvfn4>
- What Are Stents? | NHLBI, NIH. (2023, November 30). NHLBI, NIH. Retrieved from <https://www.nhlbi.nih.gov/health/stents>
- What Is Cardiac Catheterization | NHLBI, NIH. (2022, March 24). NHLBI, NIH. Retrieved from <https://www.nhlbi.nih.gov/health/cardiac-catheterization>
- What is the Aorta? (n.d.). Mount Sinai Health System. Retrieved from <https://www.mountsinai.org/care/heart/services/aortic/what-is>
- Wu, C. A., Squelch, A., & Sun, Z. (2021). Investigation of Three-dimensional Printing Materials for Printing Aorta Model Replicating Type B Aortic Dissection. *Current Medical Imaging Reviews*, 17(7), 843–849. <https://doi.org/10.2174/1573405617666210218102046>
- Sun, Z. (2020). Clinical Applications of Patient-Specific 3D Printed Models in Cardiovascular Disease: Current Status and Future Directions. *Biomolecules*, 10 (11), 1577
- Schulze, M., Juergensen, L., Rischen, R., Toennemann, M., Reischle, G., Puetzler, J., Gosheger, G., & Hasselmann, J. (2024). Quality assurance of 3D-printed patient specific anatomical models: a systematic review. *3D Printing in Medicine*, 10(1). <https://doi.org/10.1186/s41205-024-00210-5>
- Schlegel, L., Ho, M., Fields, J. M., Backlund, E., Pugliese, R., & Shine, K. M. (2022). Standardizing evaluation of patient-specific 3D printed models in surgical planning: development of a cross-disciplinary survey tool for physician and trainee feedback. *BMC Medical Education*, 22(1). <https://doi.org/10.1186/s12909-022-03581-7>

- Antonuccio, M. N., Gasparotti, E., Bardi, F., Monteleone, A., This, A., Rouet, L., Avril, S., & Celi, S. (2023). Fabrication of deformable patient-specific AAA models by material casting techniques. *Frontiers in Cardiovascular Medicine*, 10. <https://doi.org/10.3389/fcvm.2023.1141623>
- Cutugno, S., Agnese, V., Gentile, G., Raffa, G. M., Wisneski, A. D., Guccione, J. M., Pilato, M., & Pasta, S. (2021). Patient-Specific Analysis of Ascending Thoracic Aortic Aneurysm with the Living Heart Human Model. *Bioengineering*, 8(11), 175. <https://doi.org/10.3390/bioengineering8110175>
- 3D Printing Store.co.za. (2023, March 17). *Anycubic m3 max / Review* [Video]. YouTube. <https://www.youtube.com/watch?v=oKcErhAkELM>
- ANYCUBIC-US. (n.d.-a). *Anycubic Photon M3 Max - largest & finest desktop resin 3D printer for enthusiast*. <https://store.anycubic.com/products/photon-m3-max?srltid=AfmBOopkRyG7jP9qGqDJx4Wri9C5KOKcnaXfd0YK6CUkUEyvJcJjaYAc>
- ANYCUBIC-US. (n.d.-b). *Anycubic Tough Resin Ultra - unrivaled toughness and resilience for 3D prints*. <https://store.anycubic.com/products/tough-resin-ultra?srltid=AfmBOoqELidwzjsiQkwAjAavi82gn4H2Ze68yGii5kbLRRKZu7aZCP7GN>
- Athani, A., Ghazali, N. N. N., Badruddin, I. A., Usmani, A. Y., Kamangar, S., Anqi, A. E., & Ahammad, N. A. (2021). Two-Phase Non-Newtonian pulsatile blood flow simulations in a rigid and flexible Patient-Specific left coronary artery (LCA) exhibiting Multi-Stenosis. *Applied Sciences*, 11(23), 11361. <https://doi.org/10.3390/app112311361>
- Colin Klupiec. (2024a, June 25). *Anycubic Tough Resin ULTRA / How tough?* [Video]. YouTube. <https://www.youtube.com/watch?v=u6vqb5tQAGU>
- Colin Klupiec. (2024b, August 13). *Anycubic Tough Resin Ultra / Precise printing?* [Video]. YouTube. <https://www.youtube.com/watch?v=87JQsi6dI58>
- Etli, M., Canbolat, G., Karahan, O., & Koru, M. (2020). Numerical investigation of patient-specific thoracic aortic aneurysms and comparison with normal subject via computational fluid dynamics (CFD). *Medical & Biological Engineering & Computing*, 59(1), 71–84. <https://doi.org/10.1007/s11517-020-02287-6>
- Monocure3D Pro Tips. (2022, August 5). *How to setup and use the Anycubic Photon M3 Max 7K 3D printer* [Video]. YouTube. <https://www.youtube.com/watch?v=eHzz7KsLHk4>

- Park, W. K., Park, K. L., Cho, Y. S., Han, A., Ahn, S., & Min, S. (2019). Intravascular epithelioid angiosarcoma in the abdominal aorta mimicking an infected aneurysm. *Vascular Specialist International*, 35(4), 232–236. <https://doi.org/10.5758/vsi.2019.35.4.232>
- Simão, M., Ferreira, J., Tomás, A. C., Fragata, J., & Ramos, H. (2017). Aorta Ascending Aneurysm Analysis Using CFD Models towards Possible Anomalies. *Fluids*, 2(2), 31. <https://doi.org/10.3390/fluids2020031>
- Teaching Tech. (2022, May 6). *Resin 3D printing beginners step by step guide* [Video]. YouTube. <https://www.youtube.com/watch?v=UU6tWhV010M>

